PLOS ONE

RESEARCH ARTICLE

Burkholderia collagen-like protein 8, Bucl8, is a unique outer membrane component of a putative tetrapartite efflux pump in *Burkholderia pseudomallei* and *Burkholderia mallei*

Megan E. Grund[1], Soo J. Choi[1], Dudley H. McNitt[1], Mariette Barbier[1], Gangqing Hu[1,2,3], P. Rocco LaSala[4], Christopher K. Cote[5], Rita Berisio[6], Slawomir Lukomski[1,2]*

1 Department of Microbiology, Immunology and Cell Biology, School of Medicine, West Virginia University, Morgantown, WV, United States of America, **2** Cancer Center, West Virginia University, Morgantown, WV, United States of America, **3** Bioinformatics Core, West Virginia University, Morgantown, WV, United States of America, **4** Department of Pathology, West Virginia University, Morgantown, WV, United States of America, **5** Bacteriology Division, The United States Army Medical Research Institute of Infectious Diseases (USAMRIID), Frederick, MD, United States of America, **6** Institute of Biostructures and Bioimaging, National Research Council, Naples, Italy

* slukomski@hsc.wvu.edu

Citation: Grund ME, Choi SJ, McNitt DH, Barbier M, Hu G, LaSala PR, et al. (2020) *Burkholderia* collagen-like protein 8, Bucl8, is a unique outer membrane component of a putative tetrapartite efflux pump in *Burkholderia pseudomallei* and *Burkholderia mallei*. PLoS ONE 15(11): e0242593. https://doi.org/10.1371/journal.pone.0242593

Editor: Axel Cloeckaert, Institut National de la Recherche Agronomique, FRANCE

Received: September 18, 2020

Accepted: November 6, 2020

Published: November 23, 2020

Data Availability Statement: All relevant data are within the paper and its Supporting Information files.

Funding: S.L. was supported by the Vaccine Development Center at WVU-HSC, Research Challenge Grant no.HEPC.dsr.18.6 from the Division of Science and Research, WV Higher Education Policy Commission. G.H. was supported with Bioinformatics Core grants NIH-NIGMS U54 GM- 104942 and P20 GM103434 R.B.

Abstract

Bacterial efflux pumps are an important pathogenicity trait because they extrude a variety of xenobiotics. Our laboratory previously identified *in silico Burkholderia* collagen-like protein 8 (Bucl8) in the hazardous pathogens *Burkholderia pseudomallei* and *Burkholderia mallei*. We hypothesize that Bucl8, which contains two predicted tandem outer membrane efflux pump domains, is a component of a putative efflux pump. Unique to Bucl8, as compared to other outer membrane proteins, is the presence of an extended extracellular region containing a collagen-like (CL) domain and a non-collagenous C-terminus (Ct). Molecular modeling and circular dichroism spectroscopy with a recombinant protein, corresponding to this extracellular CL-Ct portion of Bucl8, demonstrated that it adopts a collagen triple helix, whereas functional assays screening for Bucl8 ligands identified binding to fibrinogen. Bioinformatic analysis of the *bucl8* gene locus revealed it resembles a classical efflux-pump operon. The *bucl8* gene is co-localized with downstream *fusCDE* genes encoding fusaric acid (FA) resistance, and with an upstream gene, designated as *fusR*, encoding a LysR-type transcriptional regulator. Using reverse transcriptase (RT)-qPCR, we defined the boundaries and transcriptional organization of the *fusR-bucl8-fusCDE* operon. We found exogenous FA induced *bucl8* transcription over 80-fold in *B. pseudomallei*, while deletion of the entire *bucl8* locus decreased the minimum inhibitory concentration of FA 4-fold in its isogenic mutant. We furthermore showed that the putative Bucl8-associated pump expressed in the heterologous *Escherichia coli* host confers FA resistance. On the contrary, the Bucl8-associated pump did not confer resistance to a panel of clinically-relevant antimicrobials in *Burkholderia* and *E. coli*. We finally demonstrated that deletion of the *bucl8*-locus drastically affects the

acknowledges funding by the project 2017SFBFER provided by the Italian MIUR.

Competing interests: The authors have declared that no competing interests exist.

growth of the mutant in L-broth. We determined that Bucl8 is a component of a novel tetrapartite efflux pump, which confers FA resistance, fibrinogen binding, and optimal growth.

Introduction

Burkholderia pseudomallei and *Burkholderia mallei* are Gram-negative bacteria that are the etiological agents of melioidosis and glanders, respectively [1]. Both pathogens are highly virulent and easily aerosolized, therefore they are classified as Tier one select agents by both the U.S. Department of Health and Human Services and the U.S. Department of Agriculture. In addition to being a biodefense concern, the bacteria are highly resistant to antibiotics and currently there is no licensed vaccine for either pathogen. Increasing global investigation into melioidosis has indicated that the disease may be more widespread than originally reported [2], and it has one of the highest disability-adjusted life years (DALYs) of neglected tropical diseases at 4.6 million [3].

B. pseudomallei is a soil saprophyte that can infect humans, resulting in symptoms ranging from localized infections, including swelling or ulcerations, to systemic infections that can lead to septic shock [4]. Treatment includes an extensive two-part chemotherapeutic regimen, most commonly using ceftazidime intravenously and then following it with an oral antibiotic eradication therapy of trimethoprim/sulfamethoxazole [5, 6]. *B. mallei* is a clonal derivative of *B. pseudomallei* that has undergone significant genomic reduction and rearrangement. This genomic evolution is attributed to the species transition from being a soil saprophyte to an obligate host pathogen, selecting for genes advantageous for host-survival [7]. Glanders primarily affects equines, but can infect other livestock such as donkeys and goats. Although uncommon in humans, this zoonotic disease is often fatal if left untreated [4]. Symptoms typically affect the pulmonary system, including pneumonia and lung abscess, but may also present as cutaneous ulceration following direct inoculation.

Several classes of efflux pumps are expressed in multidrug resistant Gram-negative bacteria, such as *Pseudomonas aeruginosa*, *Acinetobacter baumannii*, and *Burkholderia spp*., and are at least partly responsible for their intrinsic antimicrobial resistance, including resistance-nodulation division (RND) efflux pumps [8]. *Burkholderia* are notorious for being resistant to an array of antibiotics, such as β-lactams, aminoglycosides, tetracyclines, fluoroquinolones, macrolides, polymyxins, and trimethoprim [9], resulting in serious infections that are hard to treat [10]. Bioinformatic analyses of the *B. pseudomallei* genomes have identified at least ten RND efflux pumps [11], although only three systems were characterized in more detail, *e.g*., AmrAB-OprA, BpeAB-OprB, and BpeEF-OprC [12]; this gap in knowledge underscores a need for more studies of drug efflux pumps in *Burkholderia* [13]. Importantly, a large body of evidence indicates that efflux pumps also contribute to resistance to a variety of host-defense molecules, biofilm formation, regulation of quorum sensing and balanced metabolism, and overall pathogenesis [14], which further accentuate the importance of the efflux systems in bacteria.

Our previous studies have identified 13 novel *Burkholderia* collagen-like (CL) proteins (Bucl) containing collagen-like Gly-Xaa-Yaa (GXY) repeats, as well as non-collagen domains, some of which had predicted functions: Talin-1 cytoskeletal integrin-binding domain, Bac_export_1 domain found in inner-membrane protein components of a type III secretion system, or Bac_export_3 domain of solute-binding proteins often associated with ABC-type transporters [15]. Specifically, Bucl8 was predicted to be an outer membrane protein, containing tandem efflux pump OEP1 and OEP2 (outer membrane efflux protein; PF02321) domains.

Unique to Bucl8, as compared to typical outer membrane proteins with OEP domains, is the presence of an extended extracellular portion of unknown function that contains a presumed collagen-like (CL) domain, followed by a non-collagen C-terminal (Ct) region. This Bucl8 variant was present only in *B*. *pseudomallei* and *B*. *mallei*. In addition, the collagen domain, which is broadly characterized as a stretch of repeating GXY motifs [16], in Bucl8 is composed of an uncommon repeating (Gly-Ala-Ser or GAS)$_n$ collagen-like sequence.

Here, our objectives are to characterize the structure and function of the Bucl8 extracellular domain, define the *bucl8* locus, and identify substrates and potential function(s) of the putative Bucl8-associated efflux pump. We demonstrate that the collagen-like domain indeed adopts the characteristic collagen triple-helical structure. In addition, the recombinant extracellular portion of Bucl8 can bind to fibrinogen. We find that Bucl8 is the outer membrane component of an efflux pump responsible for fusaric acid (FA) resistance, a potent mycotoxin produced by *Fusarium* species that cohabitate the soil environment with *Burkholderia* [17, 18]. We further identify *bucl8*-associated genes, designated *fusCDE*, encoding the remaining components of the putative Bucl8-efflux pump. Transcripts of the *bucl8*-operon were upregulated in *B*. *pseudomallei* and *B*. *mallei* by exogenous FA, as well as by FA-derivative *p*-hydroxybenzoic acid (pHBA), which is involved in regulation of balanced metabolism in *E*. *coli*. FA resistance was diminished in a *B*. *pseudomallei* isogenic deletion mutant without the *bucl8* locus and could also be transferred to a FA-sensitive *E*. *coli* strain. Lastly, we found that the mutant grew at a significantly reduced rate, suggesting that under laboratory conditions the pump is important for the cell's physiology. Here, we describe a previously unreported putative efflux pump with unique structure and functional implications in the biology of *B*. *pseudomallei* and *B*. *mallei* species.

Materials and methods

Bacterial strains and growth

Two BSL2 *Burkholderia* strains exempt from the Select Agents list were used in this study: (i) *B*. *pseudomallei* strain Bp82 is an avirulent Δ*purM* mutant of strain 1026b [19], which was obtained from Christopher Cote (US AMRIID, Frederick, MD) and (ii) *B*. *mallei* CLH001 Δ*tonB*Δ*hcp1* mutant originates from the strain Bm ATCC23344 [20], which was obtained from Alfredo Torres (UTMB, Galveston, TX) (Table 1). Strain Bp82 was routinely grown in Luria broth-Miller (LBM) with shaking at 37˚C and on Luria agar (LA) solid medium at 37˚C. Strain CLH001 was grown under the same conditions, but the broth medium was supplemented with 4% glycerol. *E*. *coli* strains JM109 (Promega) and S17-1λpir/pLFX (*E*. *coli* Genetic Stock Center, Yale University) were cultured in LBM media and on LA. Antimicrobials were used in selective media and in susceptibility/ resistance assays, as described in the methods below.

Bioinformatic analyses of the *bucl8* locus

Annotation of transcriptional and translational signals. The promoter regions of *fusR* and *bucl8* were defined by combining public transcriptome data and computational prediction. Briefly, strand-specific RNA-Seq data of *B*. *pseudomallei* [23] was downloaded from National Center for Biotechnology Information (NCBI) Sequence Read Archive (SRA) under BioProject accession PRJNA398168. The RNA-Seq read distribution across the genome was visualized by the UCSC genome browser [24], which includes a reference strain for 1106a. The genomic region spanning genes *fusR* to *tar* is highly similar between strain Bp 1106a and our target strain Bp 1026b (identity = 99.4%). The RNA-Seq reads were pooled and then mapped to the genome of strain 1106a using Bowtie2, which allows two base-pair mismatch [25]. The

Table 1. Bacterial strains and plasmids.

Strains and Plasmids		Description/ Characteristics	Source
B. pseudomallei	Bp 1026b (genomic DNA)	Blood culture from 29-year-old female rice farmer with diabetes mellitus, Northeast Thailand, Sappasithiprasong hospital; 1993	BEI Resources
	Bp K96243 (genomic DNA)	Female diabetic patient- Khon Kaen hospital, Northeast Thailand; 1996	BEI Resources
	Bp82	Attenuated 1026b strain with a partial deletion of the *purM* gene resulting in adenine and thiamine auxotrophy	USAMRIID, Frederick, MD
	Bp82Δ*bucl8-fusE*	Bucl8-associated pump deletion mutant	This study
B. mallei	CLH001	Attenuated Bm ATCC23344 mutant with genes *tonB* (iron acquisition) and *hcp1* (type 6 secretory system structural protein) deleted	UTMB, Galveston, TX
E.coli	JM109	Host strain; Δ*endA1*, Δ*recA1*, Δ*lacZ* gene	Promega
	JM109::525	JM109 with pSL525 plasmid containing the Bucl8-pump locus from Bp 1026b/Bp82	This study
	JM109::529	JM109 with pSL529 plasmid containing the Bucl8-pump locus from Bp K96243	This study
	S17-1λpir/pLFX	Mobilization host	*E. coli* Genetic Stock Center, Yale University
Plasmids	pQE-30	*E. coli* expression vector for proteins with N-terminal 6xHis-tag; T5 promoter; ampicillin resistance	Qiagen
	pUC18T-mini-Tn7T-Tp	Mobilizable TpR mini-Tn7 vector; trimethoprim and ampicillin resistance	[21]
	pMo130	Mobilizable *E. coli* vector that is suicide in *Burkholderia*	[22]
	pSL520	pQE-30-based plasmid for expression of rBucl8-Ct protein	This study
	pSL521	pQE-30-based plasmid for expression of rBucl8-CL-Ct protein	This study
	pSL522	pMo130-based plasmid with *fusR* for generating chromosomal deletion of Bucl8-pump.	This study
	pSL524	pMo130-based plasmid with *fusR* and *tar* for generating chromosomal deletion of Bucl8-pump	This study
	pSL525	pUC18T-mini-Tn7T-Tp based plasmid with Bucl8-pump locus of Bp 1026b/Bp82	This study
	pSL529	pUC18T-mini-Tn7T-Tp based plasmid with Bucl8-pump locus of Bp K96243	This study

https://doi.org/10.1371/journal.pone.0242593.t001

RNA-Seq read density at each genomic position was visualized by the UCSC genome browser [24] to determine putative transcription boundaries of *fusR* and *bucl8*. Sigma 70 promoters (-10 and -35) were predicted by BPROM [26]. Translation initiation sites (TISs) were predicted by TriTISA with default parameters [27]. The Shine-Dalgarno (SD) translation initiation signals were manually annotated within 20 bps upstream to TISs by considering "GGAG", a SD consensus sequence annotated for *Burkholderia* [28]. The gene and protein designation were adopted according to Crutcher *et al*. 2017.

Prediction of FusR putative binding sites. The positions of the predicted FusR binding sites, a LysR-type transcriptional regulator, were determined using the University of Braunschweig Virtual Footprint Promoter analysis tool v3.0 [29]. Known LysR regulators were used as models to predict binding, including CysB, MetR, and OxyR from *E. coli*, GltC from *Bacillus subtilis*, and OxyR from *P. aeruginosa*. Standard settings were used to run the prediction (sensitivity = 0.8, core sensitivity = 0.9, and size = 5) on the 500-bp region upstream from the translational start site of *bucl8*.

Genetic and molecular biology methods

Construction of an unmarked isogenic deletion mutant of *bucl8* locus in Bp82. The chromosomal region in Bp82, encompassing genes *bucl8-fusCD-fusE*, was deleted using suicide plasmid pSL524 constructed in vector pMo130 (Addgene), as described previously [22]. Two Bp82-DNA fragments of about 1 kb each were sequentially cloned within the multiple cloning site of pMo130: (i) pSL522 construct, containing *fusR* gene located upstream of *bucl8*

was PCR-amplified with primers pSL522-ApaI-F and pSL522-HindIII-R, was cloned between *Apa*I-*Hind*III sites of the vector; and (ii) pSL524, containing *tar* gene located downstream of *fusE* was cloned at *Apa*I site, following amplification with primers pSL523-ApaI-2F and pSL523-ApaI-2R.

Plasmid pSL524 was introduced by conjugation into Bp82 via biparental mating with a donor strain *E. coli* S17-1λpir/pLFX::pSL524 on LA medium overnight. The mating bacteria were then scraped off and plated onto selective LA medium supplemented with 200 μg/mL kanamycin, to counter-select WT Bp82, and 50 μg/mL zeocin, to counter-select *E. coli*. Merodiploid colonies resulting from the single cross-over event, were sprayed with 0.45 M pyrocatechol (Sigma-Aldrich) to detect yellow transconjugants [22]. Several yellow colonies were streaked onto YT medium (10 mg/mL yeast extract, 10 mg/mL tryptone) containing 15% sucrose to force the excision of the *bucl8-fusE* locus and pMo130 sequence from Bp82 merodiploids. Colonies were grown for 48 hours. Successful excision produces deletion mutants as white colonies identified by spraying with pyrocatechol. White colonies were isolated and characterized by PCR and sequencing to confirm the deletion of the *bucl8-fusCD-fusE* genes.

Cloning of *bucl8* locus in *E. coli* JM109. The cloning strategy was based on the genomic sequence of the Bp82 parent strain *B. pseudomallei* 1026b, which identified a ~8.2-kb *Stu*I-*Stu*I fragment, encompassing the entire *fusR-bucl8-fusCD-fusE* locus. Bp82 gDNA was digested with *Stu*I and DNA species of about 8–10 kb were isolated from the gel and ligated to *Stu*I-cleaved vector pUC18T-mini-Tn7T-Tp (pUC18T-mini-Tn7T-Tp was a gift from Heath Damron, Addgene plasmid # 65024) [21].The *E. coli* JM109 transformants were isolated on a LA medium containing 100 μg/mL FA. Plasmid pSL525 was isolated from several colonies and analyzed by restriction digestion. Junctions between vector and insert sequences were sequenced to establish insert orientation. The presence of *fusR-bucl8-fusC-fusE* genes was verified by PCR and sequencing.

The plasmid construct pSL529, containing the *bucl8* sequence with extended CL region from Bp K96243, was also generated based on pSL525. An internal Bucl8 fragment from Bp K9264 (~1.4-kb) was PCR-amplified (using primers Bucl8-1F and BurkhFusBCD-1R) and cloned between two unique sites in *bucl8*, *Xcm*I, and *Fse*I, of pSL525. *E. coli* JM109 transformants were isolated on a LA medium containing 100 μg/mL ampicillin. The plasmid sequence was verified as before.

Cloning, expression and purification of Bucl8-derived recombinant proteins. Two recombinant polypeptides, derived from the presumed extracellular portions of Bucl8 variant in Bp K96243, were generated for this study: (i) pSL521-encoded rBucl8-CL-Ct polypeptide, containing both the collagen-like region and the non-collagen C-terminal region and (ii) pSL520-encoded rBucl8-Ct, which only includes the C-terminal region.

For cloning, gBlocks (Integrated DNA Technologies) were designed, encoding two recombinant constructs (S3 Table), as described [30]. gBlocks were used as templates to produce cloned DNA inserts using primers pSL521-F and pSL521-2R for pSL521 construct, and pSL520-F and pSL520-R for pSL520. gBlock DNA fragments were inserted between *Hind*III and *BamH*I sites of the pQE-30 vector, resulting in an N-terminal 6xHis-tag (Qiagen) for each construct and were then cloned into *E. coli* JM109. Plasmid constructs pSL520 and pSL521 were confirmed by sequencing (Primers pQE30-F, pQE30-2R).

For protein expression, *E. coli* JM109 with pSL520 or pSL521 constructs were grown in LBM plus 100 μg/mL ampicillin with shaking at 37°C overnight, and then 10 mL cultures were used to inoculate 1 L batches of the same media. The protein expression was induced in cultures at OD_{600} ~0.5 with 1 mM isopropyl β-d-1-thiogalactopyranoside for 3 hours and then bacterial cells were pelleted and frozen at -20˚C overnight. Cell pellets were thawed and suspended in 10 mL of lysis buffer (50 mM Tris buffer, 50 mM NaCl, 2 mM $MgCl_2$, 2% Triton X-

100, 10 mM β-mercaptoethanol, 0.2 mg/mL lysozyme, 1 mL of Protease inhibitor (Pierce), 1 mM PMSF, 10 μg/mL). The samples were vortexed, placed on ice for 20 minutes, and then centrifuged. The supernatants were applied onto affinity columns with HisPur^{TM} Cobalt Resins (Thermo Fisher Scientific) and purification was carried out according to manufacturer's protocol. The eluted proteins were analyzed by 4–20% SDS-PAGE to assess the overall integrity and purity. The proteins were dialyzed in 25 mM HEPES and stored at -20˚C.

Ligand binding assay to rBucl8-CL-Ct and rBucl8-Ct

In the initial screening assay, binding of the rBucl8-CL-Ct to different extracellular matrix (ECM) ligands was assessed by ELISA [31]. Wells were coated overnight with 1 μg of each ligand dissolved in bicarbonate buffer: collagen type I and IV (Sigma), elastin (Sigma), fibrinogen (Enzyme Research), plasma fibronectin (Sigma), cellular fibronectin (Sigma), laminin (Gibco), and vitronectin (Sigma). Next, 1 μg per well of rBucl8-CL-Ct in TBS, 1% BSA was added and incubated for two hours at 37˚C. Wells were washed with TBS and bound rBucl8-CL-Ct was detected with anti-6His-tag mouse mAb (Proteintech) in TBS-1% BSA and a secondary goat anti-mouse HRP-conjugated Ab (Jackson Immuno Research Laboratories Inc.); immunoreactivity was detected with ABTS substrate and measured spectrophotometrically at OD_{415}. Data represent the mean ±SE of three independent experiments (n = 3), each performed in triplicate wells. Concentration-dependent binding was assessed in a similar manner, however with varying concentrations (0–10 μM) of rBucl8-CL-Ct.

Structural characterization of Bucl8

Homology modelling of the periplasmic/outer membrane component of Bucl8 was performed using the software MODELLER [32] and the structure of VceC from *V*. *cholerae* as a template (PDB code 1yc9). For the collagen-like (CL) region of Bucl8, homology modelling was performed with MODELLER [32] using the high-resolution structure of a collagen-like peptide (PDB code 1k6f) [33] as a template. The Ct random coil region was generated using the Molefacture plugin of VMD [34]. Electrostatic potential surface was computed using the software Chimera [35].

Circular dichroism spectroscopy (CD) of rBucl8-derived polypeptides was performed as previously described [30]. Briefly, protein samples were dialyzed against 1x Dulbecco's phosphate buffered saline, pH 7.4. CD spectra were taken with a Jasco 810 spectropolarimeter, in a thermostatically controlled cuvette, with a path length of 0.5 cm. Data were acquired at 10 nm per minute. Wavelength scans were performed from 240 nm to 190 nm at either 25˚C or 50˚C for unfolded triple helix in rBucl8-CL-Ct construct.

Gene transcription by RT-qPCR

Duplicated bacterial cultures of Bp82 and CLH001 were grown in broth media at 37˚C with shaking till early logarithmic phase (OD_{600} ~0.4), then, FA was added to one of each culture at sub-inhibitory concentrations and incubated for one hour. Cultures were mixed with a 1:2 ratio of RNA Protect reagent, incubated for five minutes, then centrifuged and decanted. Pellets were suspended in lysing buffer (1.3 μg/μL proteinase K, 0.65 mg/mL lysozyme, TE; 10 mM Tris, 1mM EDTA, pH 7) and incubated for ten minutes. Total RNA was isolated using RNeasy Protect Bacteria Mini kit (Qiagen). TurboDNase enzyme [36] was used to remove traces of genomic DNA. RNA was either used immediately for cDNA synthesis or stored at −80˚C for no more than one week. cDNA was generated using iScript cDNA synthesis kit (Bio-Rad).

RT-qPCR was performed using SsoAdvanced Universal SYBR Green Supermix (Bio-Rad), with primers listed in S1 Table. Transcript levels were normalized to 16S rRNA [37]. Transcription fold change was calculated as relative to non-FA conditions, using the $2^{-\Delta\Delta CT}$ method. Technical and experimental replicates were done in triplicate.

Determination of antimicrobial susceptibility/resistance

Antimicrobial susceptibility by broth dilution method. Minimum inhibitory concentration (MIC) testing was performed in liquid and on solid media. Initially, Bp82 and CLH001 were grown overnight at 37˚C with shaking to inoculate fresh media with varying concentrations of FA (32 μM to 8000 μM), as described [38]. The optical density was recorded after overnight incubation and colony forming units (CFU) were calculated after plating serially diluted samples on LA media.

Antimicrobial sensitivity on agar. Strains were also tested for growth on LA media supplemented with differing concentrations of antimicrobials. Bacterial cultures were grown to an optical density of ~0.4 and plated on agar, and incubated at 37˚C for 48 hours. The following concentrations of antimicrobials were used: fusaric acid (FA), 100–800 μg/mL [39]; para-hydroxybenzoic acid (pHBA), 0.5–2.5 mg/mL [40]; and chloramphenicol (CHL), 2–32 μg/mL serially diluted [41].

Antimicrobial susceptibility in clinical laboratory. Strains were tested with antimicrobials in a clinical laboratory using Thermo Sensititre GNX3F dehydrated 96-well plates (TREK Diagnostic Systems). Bacterial cultures were grown on LA medium and cells were emulsified in sterile water to turbidity of 0.5 McFarland. The suspension was then diluted in cation adjusted Mueller-Hinton broth with TES buffer before inoculation of 100uL (approximately $5x10^5$ CFU) into each antimicrobial test well. Plates were incubated for 24 hours at 34–36˚C in a non-CO_2 incubator. Results were read and interpreted based on manufacturer's protocol and CLSI MIC interpretive guidelines. Antimicrobials tested included: amikacin, doxycycline, gentamicin, minocycline, tobramycin, tigecycline, ciprofloxacin, trimethoprim/sulfamethoxazole, levofloxacin, aztreonam, imipenem, cefepime, meropenem, colistin, polymyxin, ceftazidime, cefotaxime, ampicillin/sulbactam, doripenem, piperacillin/tazobactam, ticarcillin/clavulanate.

Antimicrobial susceptibility was also assessed by disk diffusion using the following antimicrobials: ampicillin (Am 10), ciprofloxacin (CIP 5), doxycycline (D 30), gentamycin (GM), trimethoprim/sulfamethoxazole (SXT), tetracycline (TE 30), tobramycin (NN 10), levofloxacin (LVX 5).

Statistical analysis

Statistics were performed using GraphPad Prism software for two-tailed paired Student's *t* -test, one-way and two-way ANOVA, pending the experiment. For gene expression of the *bucl8* operon in Bp82, statistical analysis was applied to log-transformed fold changes to account for the phenomena of heteroscedasticity. Significance was denoted at levels of $^{*}p \leq 0.05$, $^{**}p \leq 0.01$, $^{***}p \leq 0.001$. Error bars represent standard error measurements (SEM) with analyses based on three independent experimental repeats (n = 3), each performed in triplicate technical replicates, unless otherwise noted.

Results

Structural and functional characterization of the extended extracellular domain of Bucl8

Bucl8 is a homotrimeric molecule, with each mature monomer comprised of two tandem outer membrane efflux protein domains (OEP1 and OEP2), and a rare repetitive region

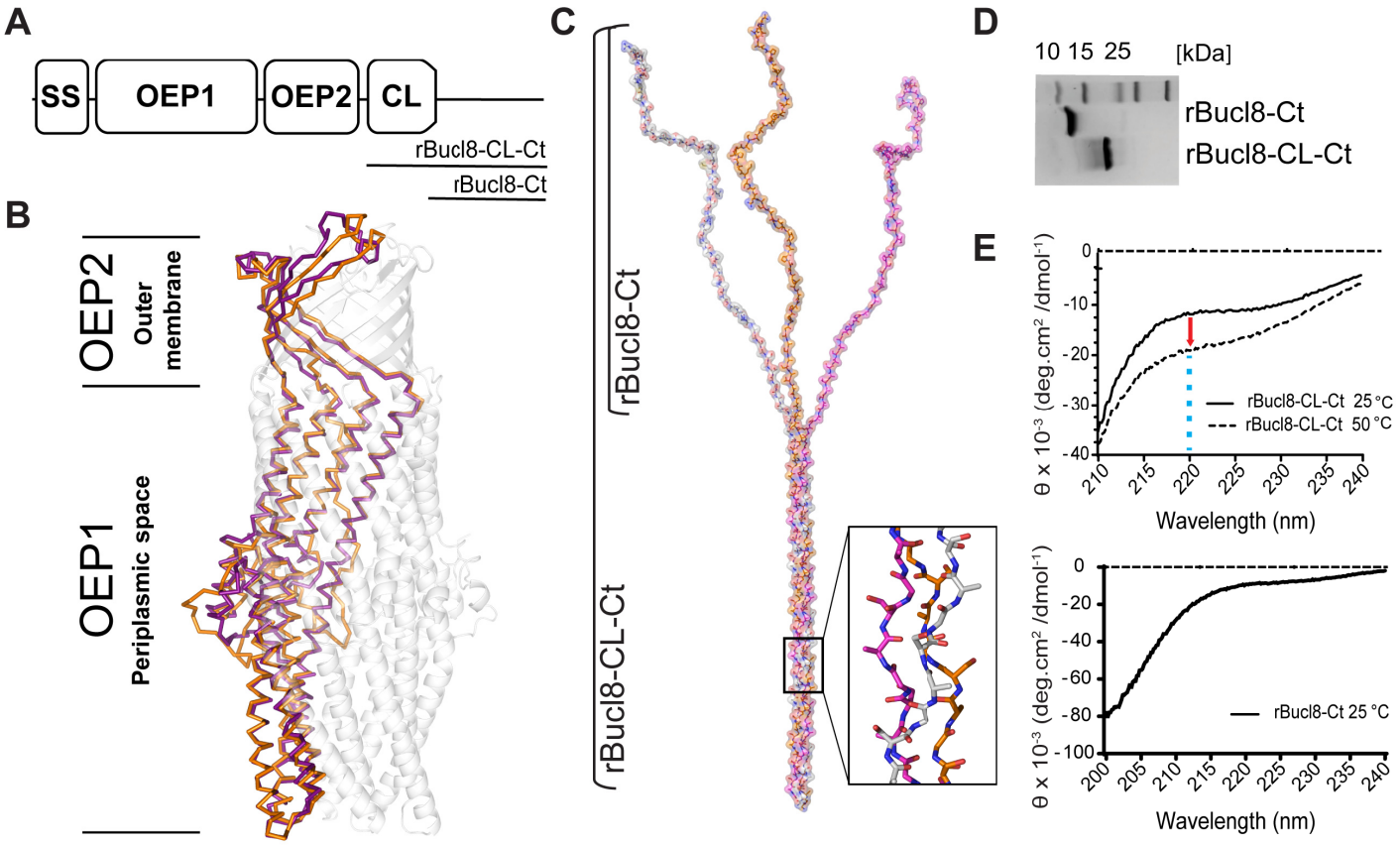

Fig 1. Structure analysis of the Bucl8 outer membrane protein. (A) Schematic organization of Bucl8 structural organization (not to scale). Bucl8 domains include: signal sequence (SS), outer membrane efflux protein domains 1 and 2 (OEP1, OEP2), collagen-like region (CL) and the C-terminus (Ct). The Bucl8 regions represented in recombinant proteins rBucl8-CL-Ct and rBucl8-Ct are depicted. (B) Homology modeling of Bucl8 intracellular OEP1-OEP2 region. Bucl8, modelled off the VceC structure (pdb code 1YC9), is shown in transparent grey. Alpha chains of Bucl8 periplasmic/outer-membrane domains (purple) superimposed onto OprM (1wp1) α-chains (orange) are shown in solid ribbon representations. (C) Structural modeling of Bucl8 extracellular CL-Ct region. Model depicts a homotrimeric polypeptide consisting of triple-helical CL domain of rBucl8-CL-Ct and unstructured C-terminus (rBucl8-Ct). The stick model in the inset depicts the triple helical fold of repeating $(GAS)_n$ collagen sequence of Bucl8-CL. (D) 4–20% SDS-PAGE analysis of recombinant Bucl8-derived constructs. rBucl8-CL-Ct and rBucl8-Ct polypeptides were expressed in *E. coli* and purified via His-tag affinity chromatography (original, uncropped gel image is shown in S1 Raw image). (E) Circular dichroism (CD) spectroscopy. (Upper plot) Wavelength scans of rBucl8-CL-Ct were performed at 25˚C (solid line) and 50˚C (dashed line). A drop in molar ellipticity maximum at 220 nm (Θ_{220}) is observed in the CD spectra, indicating the transition from triple-helical (25˚C) to unfolded form (50˚C). (Bottom plot) CD spectrum of rBucl8-Ct at 25˚C indicates an unstructured form.

https://doi.org/10.1371/journal.pone.0242593.g001

consisting of glycine, alanine, and serine $(GAS)_n$ triplet repeats, here denoted as the CL domain, which is followed by a non-collagen carboxyl-terminal (Ct) region (Fig 1A). We homology-modelled the structure of Bucl8's periplasmic/outer-membrane component, with the program MODELLER, using the crystal structure of the outer membrane channel protein VceC from *V*. *cholerae* (35.8% sequence identity; Table 2) as a template. In the homology model, the OEP1 domain is a typical α-barrel, formed by twelve short helices and six long helices, spanning the periplasmic space. The OEP2 domain forms a β-barrel, which crosses the outer membrane outwards (Fig 1B). Bucl8's homology model can be superimposed over the structure of OprM (RMSD between the two structures of 2.0 Å), which is an outer membrane component of the tripartite efflux pump complex MexAB-OprM.

Table 2. Sequence identities between Bucl8-associated efflux pump components and known corresponding proteins.

	Protein	Species	PDB code	Sequence identity (%)	Query cover (%)
Bucl8*	VceC	*Vibrio cholerae*	1YC9	35.8	63
	NodT	*Burkholderia mallei*	6U94	31.6	61
	CusC	*Escherichia coli*	3PIK	28.7	61
	OprJ	*Pseudomonas aeruginosa PAO1*	5AZS	29.9	61
	OprM	*Pseudomonas aeruginosa*	1WP1	29.0	61
	MtrE	*Neisseria gonorrhoeae*	4MT0	26.9	61
	TolC	*Escherichia coli*	1EK9	24.7	38
FusC	FuaA	*Stenotrophomonas maltophilia*		41.9	44
	AaeB	*Klebsiella pneumoniae*		24.62	60
	MexB	*Pseudomonas aeruginosa*	3W9I	NS	
	AcrB	*Escherichia coli*	4ZLJ	NS	
	CusA	*Escherichia coli*	3K07	NS	
FusD	AcrZ	*Escherichia coli*	4C48	NS	
	CusF	*Escherichia coli*	3E6Z	NS	
	YajC	*Escherichia coli*	2RDD (in complex)	NS	
FusE	MexA	*Pseudomonas aeruginosa*		30.99	48
	AcrA	*Escherichia coli*	2F1M	27.27	48
	BesA	*Borreliella afzelii*	4KKS	26.56	48
	EmrA	*Klebsiella pneumoniae*	4TKO	26.73	86
	CusB	*Escherichia coli*	3H94	NS	

NS = No significant similarity

*Comparison to Bucl8 protein sequence without CL-Ct domains.

https://doi.org/10.1371/journal.pone.0242593.t002

Following OEP2, towards the extracellular space, the trimeric structure of the molecule supports a triple-helical structure of the extracellular CL-$(GAS)_n$ domain (Fig 1C), although, the specific $(GAS)_n$ sequence has not been studied previously for triple helix formation. The number of consecutive $(GAS)_n$ repeats present fluctuates between Bucl8 variants from different *B. pseudomallei* isolates. Analysis of ~100 *bucl8* alleles showed $(GAS)_n$ numbers ranging from 6 to 38 repeats (mode: 20). Notably, 21 consecutive GAS repeats characterize the Bucl8 of *B. pseudomallei* model strain K96243, while the Bucl8 variants of the strains utilized in this study have fewer $(GAS)_n$ numbers, *e.g.*, Bp 1026b/Bp82 has six and *B. mallei* strain Bm ATCC 23344/CLH001 has eight. Following the CL-$(GAS)_n$ domain is a Ct region of 72 amino acids that are conserved among *B. pseudomallei* and *B. mallei* strains (S1 File).

Here, we homology-modelled a representative $(GAS)_{19}$ sequence using the structure of the collagen peptide $(PPG_{10})_3$ as a template (PDB code 1k6f, seqid 36%) [33] and the software MODELLER (Fig 1C). This structure formed a triple helix of about 163 Å in length. On its C-terminal end, the Ct domain of each chain is predicted by JPRED to be unfolded and was modeled in a random coil conformation (Fig 1C). Consistent with the sequence composition of the $(GAS)_n$ repetitive domain, its electrostatic potential surface appears neutral, with only a few positive charges due to the presence of arginine residues in the unstructured Ct regions of the molecule.

To experimentally validate this homology-modelled structure of the extracellular part of Bucl8, two recombinant proteins, derived from the extracellular portion of Bucl8 variant in strain Bp K96243, were designed and expressed in *E. coli*. The construct rBucl8-CL-Ct includes the CL-$(GAS)_{19}$ domain and adjacent unstructured C-terminus (Ct), while construct rBucl8-Ct encompasses the Ct region only. Both Bucl8-derived polypeptides migrate

aberrantly in SDS-PAGE in relation to molecular weight standards, *e.g.*, rBucl8-CL-Ct of expected 11.7 kDa and rBucl8-Ct of 7.8 kDa (Fig 1D). Structural analysis of rBucl8-CL-Ct rendered at 25˚C, using circular dichroism spectroscopy, confirmed a triple helical structure, demonstrated by a shallow peak at 220 nm (Fig 1E). As a control, denatured rBucl8-CL-Ct (50˚C line) displayed a further-depressed peak at 220 nm that no longer held a triple-helical collagen structure. The 220 nm peak in rBucl8-CL-Ct is less pronounced when compared to typical triple helices formed by perfect GPP collagen repeats. This feature suggests the coexistence of both triple helix and random coil structures and/or the contribution of the non-collagen Ct region to the spectrum; such effects on CD spectra were previously reported for streptococcal collagen-like rScl constructs [42]. Additionally, the rBucl8-Ct structure was also analyzed by circular dichroism spectroscopy. The absence of ellipticity maxima and/or minima of known structures, *e.g.*, α-helices or β-strands [43], indicates an unstructured protein (Fig 1E). Altogether, using *in silico* modeling and experimental CD spectroscopic analyses of the representative recombinant protein, we demonstrated that repeating $(GAS)_n$ of the predicted Bucl8-CL region from *B. pseudomallei* and *B. mallei* can form a stable collagen triple helix; to our knowledge, this is the first such demonstration obtained for the unusual repeating $(GAS)_n$ collagen-like sequence.

Bacterial proteins harboring CL domains from diverse genera have been demonstrated to bind ligands, including extracellular matrix proteins (ECM), and have been shown to participate in pathogenesis [44–46]. Here, we screened several human compounds by ELISA to ascertain a potential ligand binding function of Bucl8's extracellular region, rBucl8-CL-Ct; ligands included fibrinogen, collagen-I and IV, elastin, plasma and cellular fibronectin, and vitronectin. Of the ligands tested, rBucl8-CL-Ct construct showed significant binding to fibrinogen, but not to collagen I and elastin (Fig 2A), while binding to other ligands tested was also not significant (not shown). rBucl8-CL-Ct binding to fibrinogen-coated wells was concentration-

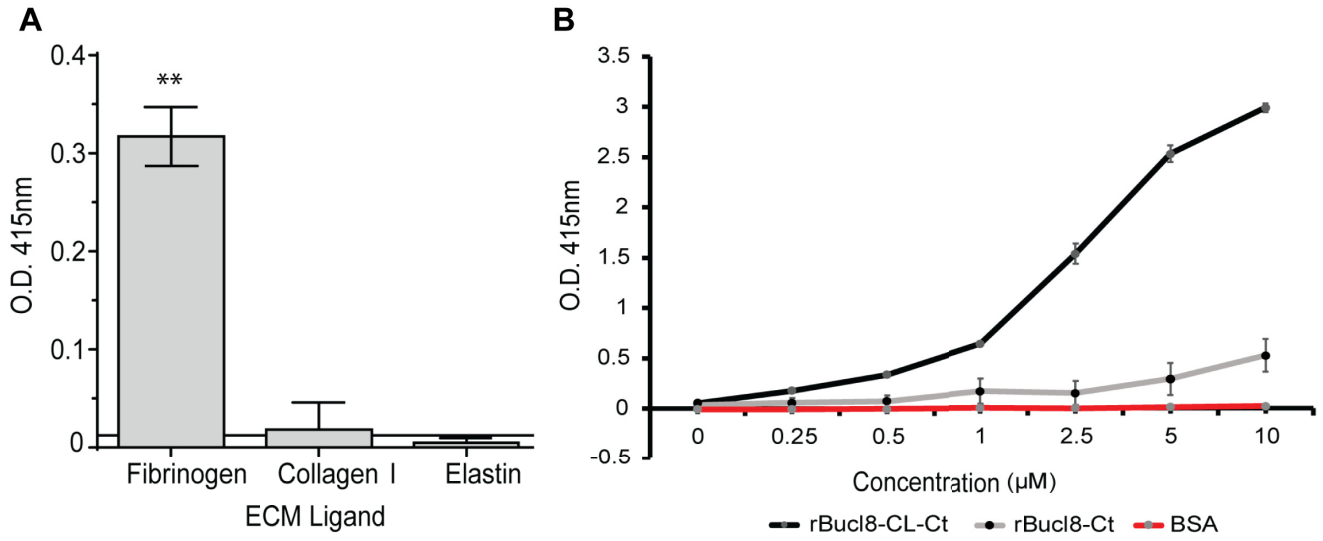

Fig 2. Binding of rBucl8-derived constructs to extracellular matrix proteins. (A) Screening assay for rBucl8-CL-Ct binding to extracellular matrix proteins. Ligand binding was tested by ELISA; representative examples of rBucl8-CL-Ct-binding-positive and binding-negative ligands are shown. rBucl8-CL-Ct binding was compared statistically with binding to BSA-coated wells plus two standard deviations; Student's *t*-test, $^{**}p \leq 0.01$. (B) Concentration-dependent binding of rBucl8-CL-Ct and rBucl8-Ct to fibrinogen. Wells were coated with fibrinogen and either recombinant Bucl8-derived protein was added at increasing concentrations. Data represents the mean ±SEM of three independent experiments (n = 3), each performed in triplicate wells. Binding was detected with an anti-His-tag mAb.

https://doi.org/10.1371/journal.pone.0242593.g002

dependent in contrast to control BSA-coated wells. In addition, rBucl8-Ct construct showed limited level of binding to fibrinogen in this assay (Fig 2B).

Identification of bucl8 operon in Burkholderia pseudomallei and Burkholderia mallei

Previously, we identified two tandem outer-membrane-efflux-protein domains in Bucl8 [15], leading to the current hypothesis that Bucl8 is the outer membrane component of an efflux pump. Genes encoding efflux pumps are often clustered in operons that are controlled in *cis* by transcriptional regulators, such as MexR of *P. aeruginosa* and AmrR of *B. pseudomallei* [47–49]. For this reason, we examined the genes surrounding *bucl8*, which are described in Table 3 and depicted in Fig 3A. The locus contains additional efflux-pump associated genes, annotated in the NCBI database to be involved in fusaric acid (FA) resistance, which we designated here as '*fus*', as previously proposed [39]. In agreement with genomic annotations, we recognize that Bucl8 is an outer membrane lipoprotein with a lipid moiety attached via the N-terminal Cys residue of the mature protein (Fig 3B; residue No. 24). In the genome of *B. pseudomallei* 1026b, downstream of *bucl8* (OMP; 594 aa) are: *fusC*, presumably encoding the inner membrane protein of the pump (IMP; 733 aa), *fusD*, encoding a small protein with domain of unknown function (DUF; 67 aa), and *fusE* encoding the periplasmic adaptor protein (PAP; 293 aa). The ATG start codon of *fusD* overlaps with a stop TGA codon of *fusC*. The direction of the next downstream gene, *tar*, is opposite to *bucl8-fusCDE* and was presumed by definition to be outside of this operon. Flanking the locus at the 5' end of *bucl8* is a divergently-oriented gene, encoding a LysR-type transcriptional regulator (LysR; 313 aa) [50], designated here as *fusR*. The proximity and opposite orientation of *fusR* gene in relation to the *bucl8-fusE* genes resembled the typical gene organization described in tripartite efflux pumps with LysR-type regulators; therefore, we hypothesized *bucl8* transcription to be regulated by the *fusR* product. Using predictive software and analysis of transcriptome data, the promoters, transcription initiation sites (TIS), and FusR binding sites were identified in the intergenic region between *fusR*

Table 3. Genes and associated identification numbers of *bucl8* locus.

		Bp 1026b			Bp K96243			Bm ATTC 23344		
Gene	**Product Annotation**	**Locus tag**	**Protein ID**	**Genomic position**	**Locus tag**	**Protein ID**	**Genomic position**	**Locus tag**	**Protein ID**	**Genomic position**
fusR	Transcriptional regulator	BP1026B_I1940	AFI66557.1	2150545–2151486	BPS_RS10485	WP_004534689.1	2345922–2346863	BMA_RS04430	WP_004191155.1	987878–988819
bucl8	RND efflux system, outer membrane lipoprotein, NodT family protein	BP1026B_I1941	AFI66559.1	2151644–2153428	BPS_RS10490	WP_162486666.1	2347036–2348973	BMA_RS04425	WP_024900385.1	985939–987705
Fusc	Fusaric acid resistance protein	BP1026B_I1942	AFI66560.1	2153445–2155646	BPS_RS10495	WP_009937757.1	2348990–2351191	BMA_RS04420	WP_004192976.1	983721–985922
fusD	Hypothetical protein	BP1026B_I1943	AFI66561.1	2155643–2155846	BPS_RS10500	WP_004191885.1	2351188–2351391	BMA_RS04415	WP_004191885.1	983521–983724
fusE	Fusaric acid resistance protein *fusE*	BP1026B_I1944	AFI66562.1	2155860–2156741	BPS_RS10505	WP_004534908.1	2351405–2352286	BMA_RS04410	WP_004191342.1	982626–983507
Tar	Methyl-accepting chemotaxis protein	BP1026B_I1945	AFI66563.1	2157092–2158768	BPS_RS10510	WP_004196082.1	2352657–2354333	BMA_RS04405	WP_004196082.1	980610–982286

Data were retrieved from NCBI for *B. pseudomallei* 1026b, *B. pseudomallei* K96243, and *B. mallei* ATTC 23344 reference genomes.

https://doi.org/10.1371/journal.pone.0242593.t003

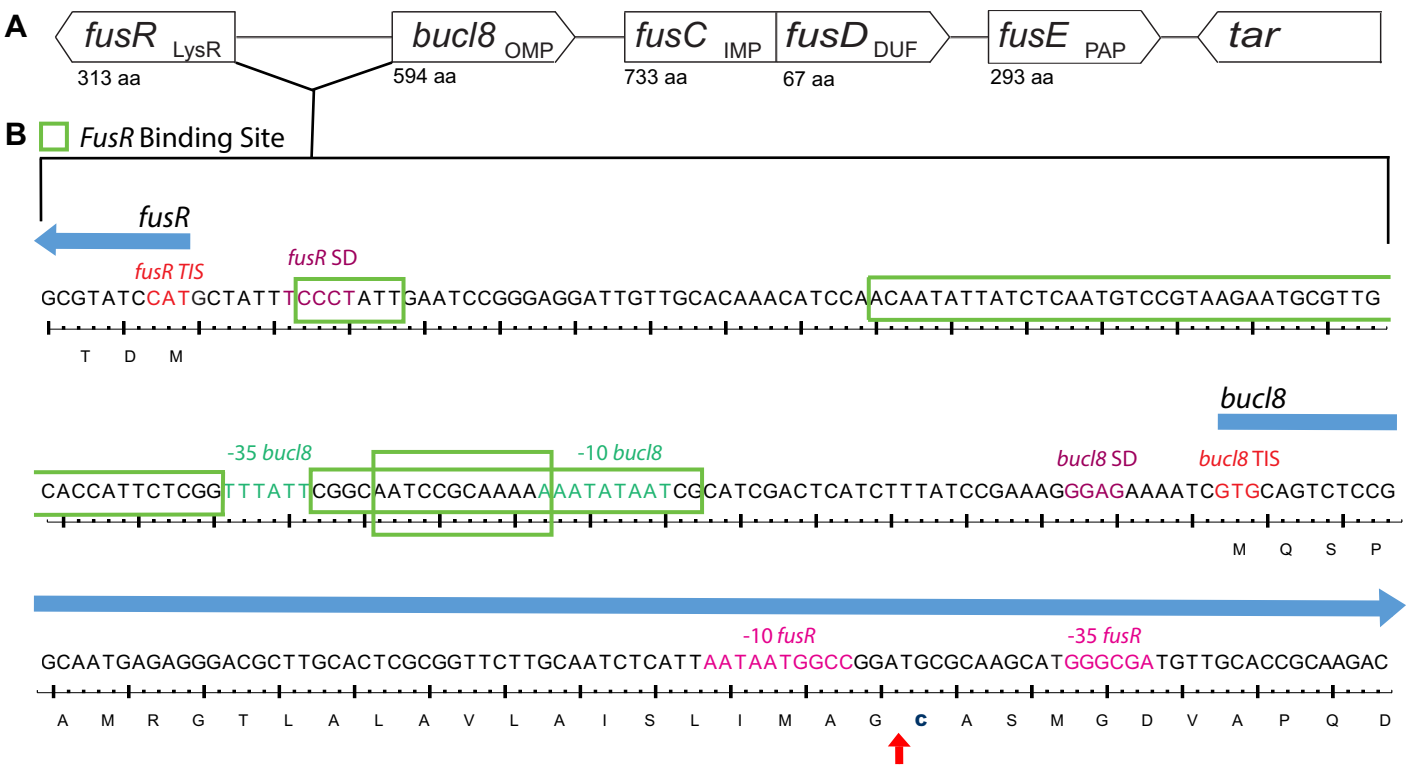

Fig 3. Chromosomal locus surrounding *bucl8* gene in *B. pseudomallei* and *B. mallei*. (A) Schematic of *bucl8*-associated locus with presumed protein function (subscript) and amino acid length (aa). Upstream of *bucl8* is gene *fusR*, while downstream are genes *fusCD* and *fusE*. Flanking the *bucl8* operon is unrelated downstream gene *tar*. LysR, LysR-type transcriptional regulator; OMP, Outer membrane protein; IMP, Inner membrane protein; DUF, Domain of unknown function; and PAP, periplasmic adaptor protein. (B) Regulatory intergenic region between *fusR* and *bucl8*. Both nucleotide and translated sequence are shown. Red arrow indicates cleavage site between the signal peptide and N-terminal cysteine linker (bolded).

https://doi.org/10.1371/journal.pone.0242593.g003

and *bucl8* (Fig 3B). FusR was predicted to have four binding sites, depicted in the green boxes that overlap with the *bucl8*–10 and -35 sites. The consensus sequence for *B. pseudomallei* is "GGAG", according to the ProTISA database [27], which matches *bucl8*'s predicted Shine-Dalgarno sequence. Thus, *fusR-bucl8-fusCD-fusE* constitute a regulon, likely involved in FA resistance. The *bucl8* locus was also conserved in Bp strain K96243 and Bm ATTC 23344; however, transcriptional units of *bucl8-fusE* were on the positive strand in the genome of K96243 strain, and on the negative strand in Bp 1026b and Bm ATTC 23344 (Table 3).

Fusaric acid increases relative expression of *bucl8*-operon transcripts

We identified a conserved operon associated with the *bucl8* gene that was present in all *B. pseudomallei* and *B. mallei* genomes analyzed, including the mutant strains Bp82 and CLH001 used in this study, and had similarity to genes encoding FA resistance found in other Gram-negative bacteria [17, 18, 39]. We consequently tested the predicted FA substrate as a transcriptional inducer for genes associated with the Bucl8-efflux pump. We first examined the FA minimum inhibitory concentration (MIC) in *B. pseudomallei* (Bp82) and *B. mallei* (CLH001) strains using a broth dilution method in the range of 32 μM FA to 8000 μM, which was based on an earlier induction data employing GFP reporter construct in *P. putida* [38]. Here, we established the FA-MIC for Bp82 as 4000 μM (716 μg/mL) and 250 μM (44 μg/mL) for CLH001.

Sub-inhibitory concentrations of FA, *e.g.*, 1000 μM for Bp82 and 60 μM for CLH001 that did not inhibit the growth rates were used in subsequent induction experiments (Fig 4A).

Total RNA was isolated from the cultures of Bp82 and CLH001 that were either non-treated or treated with FA (1000 μM or 60 μM, accordingly) at OD_{600} ~0.4 for one hour. Both *fusR* and *bucl8* genes were expressed in non-treated cultures at basal levels, but transcription of *bucl8* in Bp82 was significantly induced with FA by an average 82-fold change in relative expression and a 20-fold change of *fusR*, using $2^{\Delta\Delta}$Ct calculations (Fig 4B). CLH001 also demonstrated about a four-fold increase for *fusR* and *bucl8* when induced with 60 μM FA (Fig 4C), although this change is comparatively lower than that recorded in FA-induced Bp82.

In a following experiment we confirmed the boundaries of the *fusR-bucl8* operon by RT-qPCR. Results show that transcription levels of *fusR-bucl8-fusC-fusE* were all significantly upregulated in samples treated with FA, compared to non-treated controls (*fusR* = 20-fold ± 1.37; *bucl8* = 82-fold ± 8.73; *fusC* = 40-fold ± 2.84; *fusE* = 86-fold ± 10.65; Fig 4B). In contrast, the expression change of *tar* was significantly lower than genes from the *fusR-bucl8-fusC-fusE* operon and the associated regulatory gene *fusR* (1.5-fold ± 0.03. One-way ANOVA with Tukey's multiple comparison test of the $\log_{10}$-transformed fold change; $^{***}p < 0.001$ for all genes compared to *tar*). This is the first demonstration of FA-inducible efflux pump in *B. pseudomallei* and *B. mallei*.

A structural analog of fusaric acid pHBA induces pump expression

Previous work reported that FusC-containing FA-exuding pumps were phylogenetically related to the aromatic carboxylic acid (AaeB) pumps, although it was unknown whether AaeB systems extrude FA [39]. Notably, studies in *E. coli* show that regulated concentrations of an FA-derivative, para-hydroxybenzoic acid (pHBA), inside bacterial cells is important for balanced metabolism of the aromatic carboxylic acids [40]. Thus, we hypothesized pHBA would also increase the relative expression of the *bucl8* operon as FA did. Broth cultures of Bp82*Δbucl8-fusE* were induced with the sub-inhibitory concentration of 6.25 mM (863 μg/mL) pHBA and compared to non-treated cultures. RT-qPCR data showed in Bp82 pHBA induced a 7-fold ± 0.26 change in *fusR*, an 18-fold ± 0.78 change in *bucl8*, a 19-fold ± 0.98 change in *fusC*, and a 9-fold ± 0.52 change in *fusE*. Transcription of *tar* was not significantly affected (1.4 fold ± 0.006 change; One-way ANOVA with Tukey's multiple comparison test of the $\log_{10}$-transformed fold change; $^{***}p < 0.001$ for all genes compared to *tar*) (Fig 4D). Evidence that aromatic carboxylic acids can induce transcription of this pump may help elucidate the broader function of Bucl8-associated pump in *B. pseudomallei and B. mallei*.

Deletion of of and complementation with the Bucl8-associated pump affect sensitivity and resistance to FA and pHBA

In order to demonstrate the function of the Bucl8-pump in various physiological roles, we used a genetic approach by generating two strains for assessing (i) loss-of-function and (ii) gain-of function. For loss-of-function, we made an isogenic Bp82 mutant harboring chromosomal deletion of *bucl8-fusCD-fusE* segment, as described [22]. Plasmid pSL524 (Table 1) was constructed in the *E. coli* vector pMo130, which is suicidal in *Burkholderia*, to generate an unmarked deletion mutant (Fig 5A). Construct pSL524, carrying upstream and downstream sequences flanking *bucl8* locus was transferred to *B. pseudomallei* Bp82 via biparental mating. Deletion was achieved in a two-step insertion/excision process, as detailed in Materials and Methods section. Successful deletion of the *bucl8-fusCD-fusE* segment from the chromosome was confirmed by PCR (Fig 5B) and sequencing. We did not delete the *fusR* gene on purpose to avoid a possible global regulatory effect associated with unknown FusR function.

To exhibit gain-of function, we complemented a heterologous *E. coli* host *in-trans* with a plasmid construct pSL525 (Table 1) harboring the whole *bucl8* locus, generated in a mini-transposon

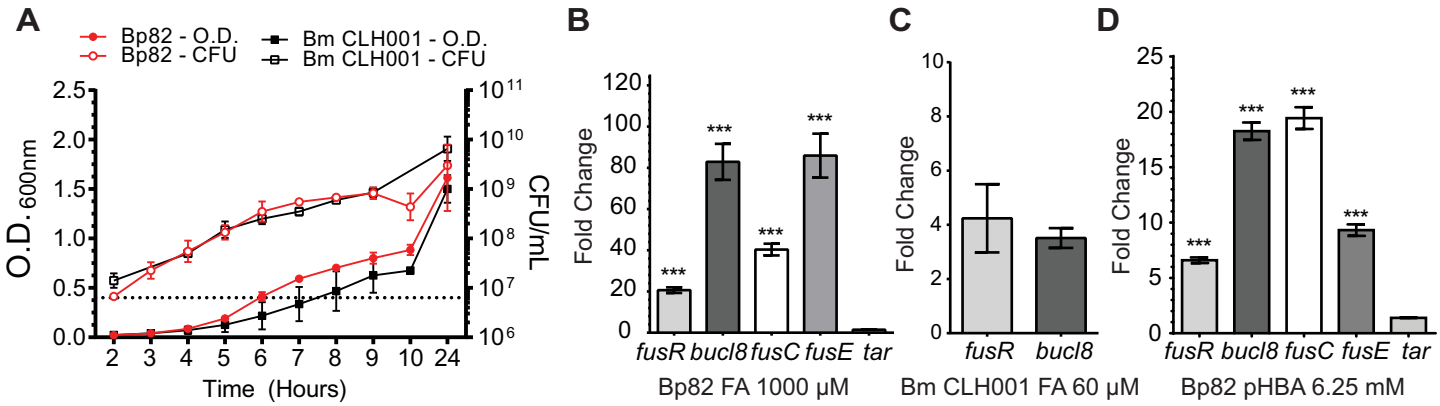

Fig 4. Effect of FA and pHBA on gene transcription within *fusR-bucl8-fusCD-fusE* operon. (A) Growth curves of *B. pseudomallei* strain Bp82 and *B. mallei* strain CLH001. Cultures were grown in strain-specific broth and optical density (O.D.) and colony forming units (CFU) were recorded. Dotted line represents OD of 0.4. Error bars represent ±SEM. (B-D) RT-qPCR was performed on RNA samples isolated from cultures of the indicated strain, untreated and treated with substrate, at an OD_{600} of ~0.4 for 1 hour. Graph shows fold change of relative gene expression compared to untreated cultures and normalized to transcription of 16S rRNA gene. Technical and experimental replicates were done in triplicate. One-way ANOVA with Tukey's multiple comparison test of the log10 –transformed fold change. Significance shown is in comparison to *tar*; $^{***}p < 0.001$. Error bars represent ±SEM. (B) Transcription activation of *fusR-bucl8-fusCD-fusE* genes in Bp82 with 1000 μM FA. The downstream *tar* gene is assumed outside of the *fusR-bucl8* operon. (C) Transcription activation of *fusR* and *bucl8* in CLH001 with 60 μM FA. (D) Transcription activation of Bucl8 regulon in Bp82 with 6.25 mM pHBA.

https://doi.org/10.1371/journal.pone.0242593.g004

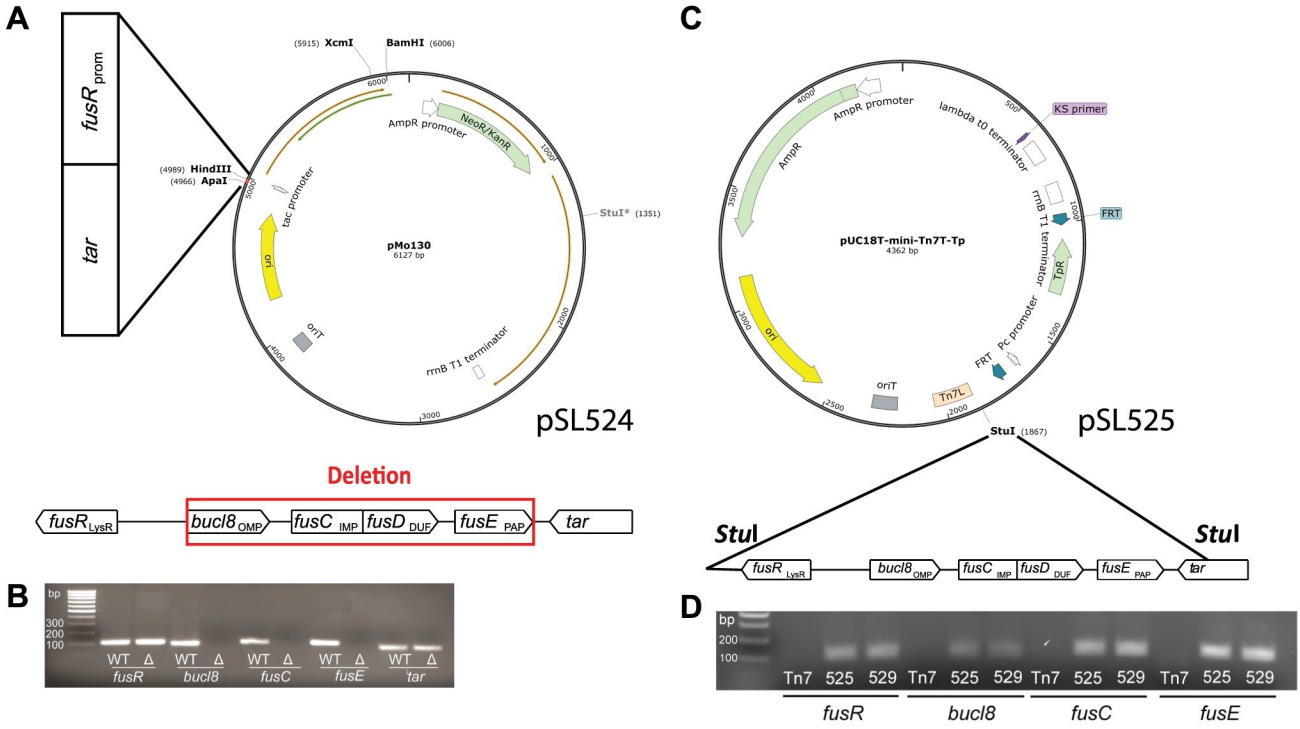

Fig 5. Construction of an unmarked Bucl8-associated pump deletion mutant and complementation in a heterologous host. (A) Strategy for generating an unmarked Bucl8-pump deletion mutant. Construction of the suicide plasmid construct pSL524. Vector pMo130, which is suicide in *Burkholderia*, was used to generate pSL524 plasmid construct for mutagenesis. *Hind*III and *Apa*I sites were utilized to clone flanking regions containing *fusR* and *tar* sequences to delete the *bucl8-fusE* coding region, depicted below. (B) Analysis of the *bucl8-fusE* deletion mutant of Bp82 by PCR. The presence of *bucl8-fusE* genes was tested in the genomic DNA isolated from wild type Bp82 (WT) and Bp82 *bucl8-fusE* mutant (Δ). (C) Cloning of the Bucl8-pump locus for *in-trans* complementation in *E. coli*. Vector pUCT18T-mini-Tn7T-Tp was used for cloning of an 8.2-kb genomic Bp82 fragment, flanked by *Stu*I sites, encompassing *bucl8* locus. (D) Characterization of the pSL525 and pSL529 constructs. The presence of *fusR-fusE* genes on pSL525 and pSL529 plasmids was tested by PCR. PCR products shown in B and D were analyzed on 1.3% agarose gel.

https://doi.org/10.1371/journal.pone.0242593.g005

vector pUC18T-mini-Tn7T-Tp, as depicted in Fig 5C. JM109::525 transformants were selected on agar containing 100 μg/mL FA and cloning was verified by PCR (Fig 5D) and sequencing. Since Bp82 represents the 1026b strain harboring Bucl8 variant with $(GAS)_6$ repeats in the CL region, we made an additional construct, pSL529, that contains $(GAS)_{21}$ repeats, to represent the majority of *B. pseudomallei* strains, by extending the number of GAS triplets in pSL525.

MICs were determined for bacterial growth on LA plates containing FA or pHBA chemicals, ranging from 0 to 800 μg/mL FA and 500–2,500 μg/mL pHBA (Fig 6A). There was a 4-fold decrease in MIC to FA from 400 μg/mL to 100 μg/mL recorded for Bp82*Δbucl8-fusE* mutant compared to the parental Bp82 strain. A similar effect was observed for pHBA; the MIC for Bp82 was 1500 μg/mL which decreased to 1000 μg/mL in the mutant. A 12-fold increased MIC on the LA medium with FA was recorded in *E. coli* JM109::525 and JM109::529 (MIC = 300 μg/mL) compared with the JM109 (MIC = 25 μg/mL) recipient. Interestingly, complementation with whole Bucl8-associated pump, however, did not increase the MIC for pHBA above 1000 μg/mL for JM109::525 or JM109:529 strains.

Although deletion of the Bucl8-associated pump resulted in a drastically decreased MIC, Bp82Δ*bucl8-fusE* mutant still maintained residual level of FA resistance (100 μg/mL). Therefore, we hypothesized that additional proteins annotated as FusC are contributing to the remaining FA resistance recorded in the Bp82Δ*bucl8-fusE* mutant. Within Bp 1026b and K96243 genomes, there are six genes present that are annotated as FusC-type proteins (Pfam #PF04632), including the protein arbitrarily designated as FusC, which is associated with Bucl8, whereas remaining five were designated FusC 2 thru FusC 6 (S2 Table). These protein sequences ranged roughly in three different lengths: ~200 amino acids for FusC 3, ~350 for FusC 4 and 6, and ~750 amino acids for FusC, FusC 2 and FusC 5. Upon examination, the loci around FusC genes 2 thru 6 were not arranged in as discernable tripartite-pump operons, like FusC, although some were adjacent to either a MFS transporter protein or genes encoding amino acid permeases. To test whether these genes are regulated by FA addition, we performed RT-qPCR on RNA isolated from Bp82 cultures induced with 1000 μM FA and without treatment. The transcription of *fusC* 2–6 genes showed little to no fold-change (0–2-fold; Fig 6B) when compared to non-treated samples, which contrasts with ~40-fold difference in *fusC* transcription (Fig 4B). Thus, we conclude that these *fusC* genes are not inducible by FA.

Bucl8-associated pump does not contribute to the Multidrug Resistance (MDR) phenotype

Efflux pumps contribute to MDR in Gram-negative bacteria [13], including *Burkholderia* species [9], and are often polyspecific [51]. A study in *S. maltophilia* concluded that an FA efflux pump did not extrude the antimicrobials tested [52]. Here, we assessed changes in resistance/susceptibility levels between Bp82 and Bp82*Δbucl8-fusE*, and JM109 and JM109::525 or JM109:529 against variety of antimicrobials.

In the clinical laboratory setting, the *Burkholderia* failed to grow in commercial medium, and therefore only the *E. coli* data were generated. Overall, there was not a significant increase in resistance to any of the antibiotics tested; JM109::525/529 showed only increased resistance to the β-lactam antibiotics, which was associated with the resistance gene present on the inserted plasmid. A disc diffusion test, including ampicillin, ciprofloxacin, levofloxacin, tobramycin, gentamicin, tetracycline, doxycycline, and trimethoprim-sulfamethoxazole, resulted in similar zones of inhibition for both Bp82 and Bp82Δ*bucl8-fusE* cultures, as well as *E. coli* JM109 and JM109::525/529, again with the exception of the plasmid-derived β-lactam resistance determinant.

Microarray data comparing the effect of 84 growth conditions on *B. pseudomallei* transcriptome showed that chloramphenicol (CHL), which contains an aromatic ring in its structure,

A

Bacteria	FA (μg/mL)	pHBA (μg/mL)	CHL (μg/mL)
Bp82	400	1500	8
Bp82Δ*bucl8-fusE*	100	1000	8
JM109	25	1000	8
JM109::525	300	1000	8
JM109::529	300	1000	8

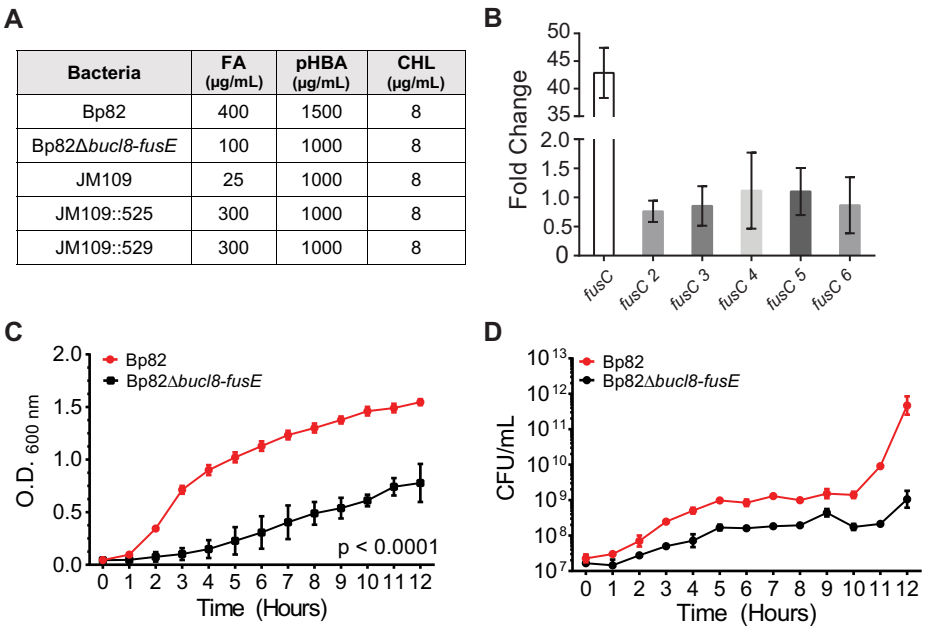

Fig 6. Analysis of loss-of-function and gain-of-function associated with chromosomal deletion and *in-trans* complementation of Bucl8-pump components. (A) Changes in sensitivity/resistance patterns in bacterial strains. MIC was determined by plating bacteria on LA containing each substrate. FA, fusaric acid; pHBA, para-hydroxybenzoic acid; CHL, chloramphenicol. (B) Relative expression of *fusC* genes. RT-qPCR was performed on total mRNA isolated from non-treated and FA-treated (1000 μM, 1 hour) Bp82 cultures (OD_{600} ~0.4). Graph shows fold change of relative gene expression compared to untreated cultures and normalized to 16S rRNA. Technical and experimental replicates were done in triplicate. (C-D) Effect of chromosomal deletion on growth. Parental strain Bp82 and its *bucl8-fusE* deletion mutant (Bp82D*bucl8-fusE*) were grown in LBM broth at 37˚C with shaking. Changes in OD_{600} (C) were recorded and CFU numbers (D) by plating on LA medium every hour. Data represents the average of three biological replicates. 2-way AVOVA with Tukey multiple comparison test, $^{***}p < 0.001$. Error bars represent ±SEM.

https://doi.org/10.1371/journal.pone.0242593.g006

induced *bucl8* expression, thus, implying CHL might be a substrate for Bucl8-associated pump [53]. Here, we determined the CHL-MICs of our *B. pseudomallei* and *E. coli* strains using a growth assay on the LA medium; however, the MIC for all the strains was the same (8 μg/mL; Fig 6A). In addition, the exogenous CHL at 8 μg/mL or 4 μg/mL concentrations did not significantly induced the transcription of *bucl8*-associated genes (not shown). Thus, our results indicate the Bucl8-associated pump is not needed for CHL resistance in *B. pseudomallei* [52].

Deletion of Bucl8-associated pump components affects cell growth

Efflux pumps extrude a variety of compounds that are toxic to the cells and play physiological functions linked to pathogenesis [14]. We observed the growth of the BpΔ*bucl8-fusE* mutant was considerably reduced than that of the parent Bp82 and did not reach the same OD_{600} in the stationary phase (Fig 6C). CFU for Bp82 increased by approximately four logs, while the mutant increased by two logs from hour 0 to 12. (Fig 6D). These results suggest that the pump components are needed for normal growth physiology under laboratory conditions in rich medium.

Discussion

The protein Bucl8 was previously predicted to be the outer membrane protein in *B. pseudomallei* and *B. mallei*. Comparative genomics studies between *B. mallei* and *B. pseudomallei* have suggested that conserved genes between the species are likely critical for host-survival,

while genes useful for saprophytic life-style and adaptability were selected against [7]. The presence of the *bucl8* genes, in particular the acquisition and conservation of the extracellular Bucl8-CL-Ct domain, in *B. pseudomallei* and *B. mallei* suggests that these genes are selected for because they are useful for bacterial survival in both the environment and in the host. Here, we carried out structure-function studies of the Bucl8 protein and the role of the putative Bucl8-associated efflux pump in antimicrobial resistance, ligand binding, and cell physiology of *B. pseudomallei* and *B. mallei* (Fig 7).

Bucl8 is a homotrimeric protein that spans the periplasmic and outer membrane to reach the extracellular region of the cell. Crystal structures of the membrane-spanning region have been reported for a number of homologous proteins, including VceC and OprM (Table 2). Superposition of the homology model of Bucl8, with the crystal structure of OprM from *P. aeruginosa* shows a strong structural conservation of both OEP1 and OEP2 domains, with root mean square deviation (RMSD) between the two structures of 2.0 Å (Fig 1B). Full structural conservation of all helices of OEP1 provides similar dimensions of the middle bulge of the OEP1 domain that accommodates substrates and suggest a similar mechanism of funnel-channel-structure mediated transport across the outer membrane.

The most puzzling feature of Bucl8 is the extracellular portion, which embeds a collagen like triple helix. In the absence of hydroxyprolines that stabilize the triple helical structure of mammalian collagen, bacterial collagens adopt alternative stabilization mechanisms to form stable triple helices [54]. While some prokaryotic collagens utilize a variety of GXY-repeat types, such as streptococcal collagen-like proteins Scl1 and Scl2 [55], others possess a limited number of triplets, including *Bacillus* Bcl proteins [56, 57]. The CL regions of various Bucl proteins utilize relatively few distinct triplet types [15]. An extreme case is the Bucl8-CL region, which is exclusively made of a rare repeating $(GAS)_n$ sequence. Our results are consistent with studies of triple helix propensity based on host-guest peptide studies, showing reasonable propensities of $(GAS)_n$ triplets to form triple helical structures. The Tm value of $(GAS)_n$ tripeptide unit in a triple helix is 33.0˚C, compared to 47.3˚C of $(POG)_n$ tripeptide (O is hydroxyproline), although, the physical anchoring of a CL domain increases Tm by additional 2˚C [58]. This relatively low Tm may suggest structural flexibility of the Bucl8 extracellular domain under physiological conditions, thus, allowing efflux pump for dual function.

Our laboratory and others have shown that bacterial collagen-like proteins participate in pathogenesis via a variety of functions, including immune evasion, cell adhesion, biofilm formation, and autoaggregation [44–46, 59]. Here, we report that the recombinant rBucl8-CL-Ct polypeptide binds to fibrinogen significantly better than rBucl8-Ct polypeptide. A similar phenomenon was recently reported for Scl1, where the effective binding to fibronectin, directly mediated by the globular V domain, required the presence of adjacent Scl1-CL domain [30]. Fibrinogen is a circulating glycoprotein that is involved in blood clotting and promoting wound healing [60]; we do not know the location of Bucl8 binding site on this multidomain protein. In the scope of pathogenesis, some Gram-negative and Gram-positive bacteria use fibrinogen for biofilm formation and bacterial adhesion. For example, fibrinogen-binding factors and clumping-factors of *Staphylococcus aureus* have been shown to increase adherence and virulence [61–63]. *B. pseudomallei* and *B. mallei* both cause cutaneous infections that lead to lesions and nodules, thus binding to wound factors could increase colonization. In addition, it is likely that unidentified ligand(s), other than fibrinogen, may exist in the environment to support a saprophytic lifestyle of *B. pseudomallei*.

bucl8-operon expression is regulated by a LysR-type transcriptional regulator, designated here as $FusR_{LysR}$. LysR-type family regulators are the most abundant class of the prokaryotic transcriptional regulators that monitor the expression of genes involved in pathogenesis, metabolism, quorum sensing and motility, toxin production, and more physiological and

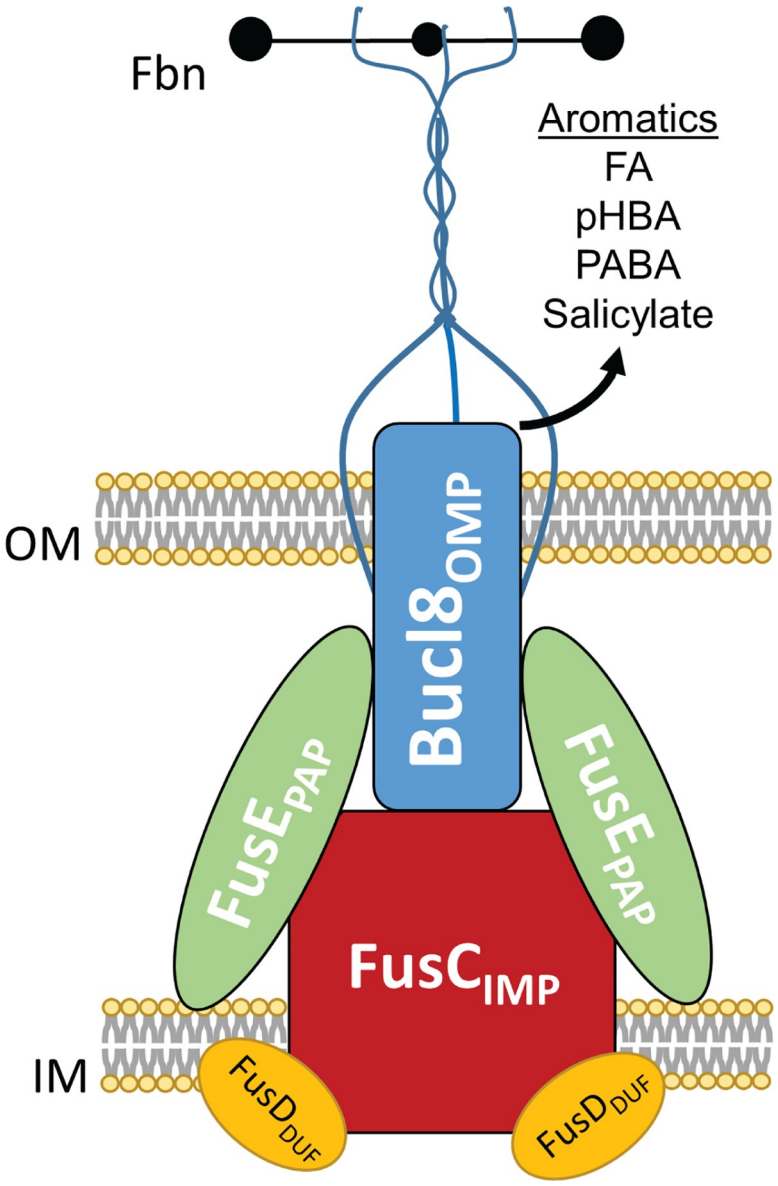

Fig 7. Model of assembled Bucl8-associated efflux pump components and substrates. Cartoon representation of assembled the Bucl8-associated efflux pump components: $Bucl8_{OMP}$, $FusC_{IMP}$, $FusD_{DUF,}$ and $FusE_{PAP}$. The extended CL-Ct structure is predicted to transverse the outer membrane into the extracellular space and to bind fibrinogen (Fbn). Aromatic substrates, such as experimentally-confirmed fusaric acid (FA) and *p*-hydroxybenzoic acid (pHBA), as well as putative *p*-aminobenzoic acid (PABA) and salicylate, are shown. OM; outer membrane. IM; inner membrane.

https://doi.org/10.1371/journal.pone.0242593.g007

virulence traits [50]. LysR proteins are tetrameric and consist of two dimers that bind and bend the DNA within promoter regions, thus, affecting the gene transcription. After the co-inducer binds to the LysR dimers, the DNA is relaxed, allowing one dimer to come into contact with the RNA polymerase to form an active transcription complex. In this study, the FusR binding sites were identified within the intergenic promoter region between *bucl8* and *fusR* in *B*. *pseudomallei* and *B*. *mallei*. Thus, we hypothesized that FA can act as a co-inducer for the *bucl8*-operon.

We show that exogenous fusaric acid (FA) induces the transcription of the *fusR-bucl8--fusCD-fusE* operon, therefore, confirming Bucl8 is a component of a previously unreported FA-inducible efflux pump in *B*. *pseudomallei* and *B*. *mallei*. Similarly, an inducible FA tripartite efflux pump, encoded by *fuaABC* operon, was identified in another soil saprophyte *S*. *maltophilia* [52]. However, the gene/protein arrangement, *e.g*. sequence orientation and length, places the *bucl8* operon within clade III of a phylogenetic tree of predicted FusC-associated operons, while *fuaABC* operon is in clade IV [39]. In addition to FA, the FA-derivative pHBA also induced the expression of the *bucl8* operon. Interestingly, although the genes and intergenic regions are highly similar, transcription of *fusR* and *bucl8* in FA-induced *B*. *mallei* culture is considerably reduced compared to *B*. *pseudomallei*. Likewise, the MIC levels for FA and pHBA were lower in *B*. *mallei*, although the *bucl8* loci are conserved between *B*. *pseudomallei* 1026b and *B*. *mallei* ATCC23344. There may be other factors affecting transcription, such as additional regulatory circuits for processing FA and similar compounds in both organisms. For similarity, another efflux pump in *B*. *pseudomallei*, BpeEF-OprC, is regulated by two highly similar LysR-type transcriptional regulators, BpeT and BpeS [64]. Further studies are needed to identify if there are other regulators or environmental stress/factors that could be affecting upstream/downstream targets.

Efflux systems are categorized into families by sequence similarity, structure–including protein fold, conserved domains, and number of transmembrane spanning regions–as well as by their energy source and substrates [65]. It is not known whether the Bucl8-associated pump relies on ATP hydrolysis to transport FA, but the associated $FusC_{IMP}$ transporter does not contain an ATP-binding domain, therefore, it is an unlikely an ABC-type transporter. In *Fusarium*, the synthesized intracellular FA is extruded by a predicted MFS-type transporter FUBT [66]. MFS transporters are typically single-component transporters, such as LacY, QacA or NorA [67, 68]; however, some MFS proteins partner with outer membrane and periplasmic adaptor components to form tripartite complexes, such as that of EmrA-EmrB-TolC in *E. coli* [69]. FusC (733 aa) is likely not an MFS transporter because it is larger than the typical length of MFS proteins (400–600 aa), does not contain well-conserved MFS motifs [68], and as we show is a component of a tetrapartite operon. Furthermore, phylogenetic analysis of bacterial efflux systems implied that FuaABC tripartite FA efflux pump in *S*. *maltophilia* forms a separate branch from other bacterial efflux pump families, branching off between the ABC and RND families [52]; of note, the Bucl8-associated FusC in B. pseudomallei and B. mallei has a 41.9% sequence identity to FuaA (Table 2). For these reasons, we think that the Bucl8-associated efflux pump is similar to an RND-type complex.

Here, we adopted the gene designation proposed by Crutcher *et al*., which also includes a fourth pump component, a small polypeptide DUF, for the Bucl8-associated tetrapartite efflux system. This situation might be more common among known tripartite efflux pumps than currently acknowledged; for example, small polypeptides YajC and AcrZ were reported as accessory components of the "tripartite" RND system AcrAB-TolC [70–72]. Another known tetrapartite RND efflux system is the CusCFBA complex, which transports heavy metals copper and silver [73]. In this system, the small CusF component serves as a periplasmic metal-binding chaperone, which hands over the metal-ion substrate to the IMP transporter [74, 75]. The precise cellular location and function of $FusD_{DUF}$ protein is not known at present.

Early studies reported FA-detoxification genes found in *Burkholderia* (formerly *Pseudomonas*) *cepacia* and *Klebsiella oxytoca* [17, 18], which were attributed to FA resistance. More recent work identified a tripartite FA efflux pump, FuaABC, in *Stenotrophomonas maltophilia* [52], while other work distinguished a large number of the phylogenetically related FusC-type proteins, conferring FA resistance, in numerous Gram-negative bacterial species [39]. Not all FusC proteins were predicted components of FA efflux pumps; however they were assumed to

be contributing to high levels of FA resistance in some species, including *Burkholderia*. Crutcher *et al*. reported positive correlation between the number of putative FusC proteins in bacterial genomes and the level of resistance to FA; for example, *Burkholderia cepacia*, harboring six predicted FusC proteins, had a FA-MIC of ≥500 μg/mL, whereas *Burkholderia glumae* had two FusC proteins and a FA-MIC of 200 μg/mL [39]. Strains with 0–1 *fusC* genes were sensitive to FA with MIC <50 μg/mL. We also observed that our Bp82Δ*bucl8-fusE* mutant retained 100 μg/mL residual resistance to FA. Through transcriptional analysis, we found that the five *fusC*/FusC genes/proteins outside of the Bucl8-operon showed little to no induction, indicating that the Bucl8-associated efflux pump is the main contributor to FA resistance in *B. pseudomallei*.

The multidrug resistance in *B. pseudomallei* is substantially attributed to previously studied RND efflux pumps BpeAB-OprB, AmrAB-OprA, and BpeEF-OprC. At the same time, little is known about the role of FA pumps in resistance against clinically used drugs. In our studies, we assessed the role of Bucl8-associated pump in multidrug resistance in two ways: (i) we compared the spectrum of resistance between parental strain Bp82 and Bucl8-pump deletion mutant, and (ii) we expressed the *bucl8*-operon in a sensitive *E. coli* strain. Although MICs for FA changed as predicted, deletion of the Bucl8-pump did not affect MIC values for the clinically-used drugs. This result is comparative to an FA pump in *S. maltophilia*, which did not determine the resistance to a large panel of therapeutics tested [52]. At the same time, a different study in the same organism showed that deletion of the *pcm-tolCsm* operon, encoding a different efflux pump, resulted in decreased MICs for several antimicrobials of diverse classes (β-lactams, chloramphenicol, quinolone, tetracycline, aminoglycosides, macrolides), and also decreased FA resistance [76]. Microarray data suggested *bucl8* expression was upregulated in the presence of chloramphenicol [53] and deletion of the *tolCsm* in *S. maltophilia* resulted in decreased resistance to both CHL and FA [76]. Both CHL and FA harbor aromatic rings in their structures, however, our investigations did not detect *bucl8*-operon induction by CHL nor changes in CHL resistance levels in Bp82Δ*bucl8-fusE* mutant or complemented *E. coli*. Altogether, we cannot exclude a possibility that redundant efflux systems are responsible for a lack of change in the drug resistance we recorded in both the *Burkholderia* isogenic mutant and complemented *E. coli*. Additional experiments will be needed, employing defined efflux-pump-deletion mutants in both hosts, to fully verify our conclusions presented here.

Efflux pumps support physiological functions [65]. The decrease in bacterial growth of the Bp82*Δbucl8-fusE* mutant suggests that the Bucl8-associated pump may be involved in modulating essential cellular stresses, both in the environment and in infected human host [14]. Limited studies show that FA repressed quorum sensing genes, expression of stress factors, secretion of siderophores, production of anti-fungal metabolites, and iron uptake [77–80]. Additionally, Bucl8-associated pump may be involved in transport of aromatic carboxylic acid compounds and act as a pHBA-metabolic efflux valve [40]. Other possible substrates include *p*-aminobenzoic acid (PABA), which is a key component of folate synthesis or salicylate, used in foods and pain-relieving drugs. (Fig 7). Ongoing investigations are aimed to define spectrum specificity of the Bucl8-associated efflux pumps in the context of the human host.

In summary, we conclude that Bucl8 is a component of a previously unreported tetrapartite efflux system that is involved in FA resistance and cell physiology. We have demonstrated that the extracellular Bucl8-CL domain forms the prototypic collagen triple-helix, while the extracellular Bucl8-CL-Ct portion is capable of binding to fibrinogen. Further studies will investigate what role fibrinogen binding plays in pathogenesis. While the Bucl8-pump is likely not be involved in the MDR phenotype of *Burkholderia*, we have identified FA and pHBA as inducible substrates of the pump and will continue to investigate metabolite analogs that may affect cell function. Importantly, the growth of the Bucl8-pump deletion mutant was significantly

affected even in the absence of FA and pHBA. By characterizing the Bucl8-associated efflux system, we can advance therapies and strategies for combating these pathogens, including developing pump inhibitors, targeting transport mechanisms, or identifying potential surface-exposed vaccine targets derived from Bucl8.

Supporting information

S1 Table. Primers.
(DOCX)

S2 Table. Genes and associated identification numbers of FusC loci.
(DOCX)

S3 Table. gBlock inserts for construction of recombinant proteins.
(DOCX)

S1 File. *bucl8* allele variants.
(XLSX)

S1 Raw image. Uncropped and unadjusted SDS-PAGE gel of purified rBucl8-Ct and rBucl8-CL-Ct constructs from Fig 1D.
(PDF)

Acknowledgments

We would like to thank Heath Damron for providing us pUC18T-mini-Tn7T-Tp vector, Alfredo Torres for providing *B. mallei* CLH001, Shelby Bradford for her assistance with initial experiments, and Paul Feustel for advice with statistical analyses. Opinions, interpretations, conclusions, and recommendations are those of the authors and are not necessarily endorsed by the US Army.

Author Contributions

Conceptualization: Megan E. Grund, Slawomir Lukomski.

Investigation: Megan E. Grund, Soo J. Choi, Dudley H. McNitt, Mariette Barbier, Gangqing Hu, P. Rocco LaSala, Rita Berisio, Slawomir Lukomski.

Project administration: Slawomir Lukomski.

Resources: Christopher K. Cote.

Writing – original draft: Megan E. Grund, Mariette Barbier, Gangqing Hu, P. Rocco LaSala, Rita Berisio, Slawomir Lukomski.

Writing – review & editing: Soo J. Choi, Dudley H. McNitt, Christopher K. Cote.

References

1. Currie BJ. *Burkholderia pseudomallei* and *Burkholderia mallei*: melioidosis and glanders. Mandell, Douglas and Bennett's Principles and Practice of Infectious Diseases 7th edn Philadelphia: Churchill Livingstone Elsevier. 2010:2869–85.
2. Limmathurotsakul D, Golding N, Dance DA, Messina JP, Pigott DM, Moyes CL, et al. Predicted global distribution of *Burkholderia pseudomallei* and burden of melioidosis. Nat Microbiol. 2016; 1:15008. https://doi.org/10.1038/nmicrobiol.2015.8 PMID: 27571754.
3. Birnie E, Virk HS, Savelkoel J, Spijker R, Bertherat E, Dance DAB, et al. Global burden of melioidosis in 2015: a systematic review and data synthesis. Lancet Infect Dis. 2019; 19(8):892–902. Epub 2019/07/

10. https://doi.org/10.1016/S1473-3099(19)30157-4 PMID: 31285144; PubMed Central PMCID: PMC6867904.

4. Nathan S, Chieng S, Kingsley PV, Mohan A, Podin Y, Ooi MH, et al. Melioidosis in Malaysia: Incidence, clinical challenges, and advances in understanding pathogenesis. Trop Med Infect Dis. 2018; 3(1). https://doi.org/10.3390/tropicalmed3010025 PMID: 30274422; PubMed Central PMCID: PMC6136604.
5. Inglis TJ. The treatment of melioidosis. Pharmaceuticals (Basel). 2010; 3(5):1296–303. https://doi.org/10.3390/ph3051296 PMID: 27713302; PubMed Central PMCID: PMC4033981.
6. Dance D. Treatment and prophylaxis of melioidosis. Int J Antimicrob Agents. 2014; 43(4):310–8. Epub 2014/03/13. https://doi.org/10.1016/j.ijantimicag.2014.01.005 PMID: 24613038; PubMed Central PMCID: PMC4236584.
7. Losada L, Ronning CM, DeShazer D, Woods D, Fedorova N, Kim HS, et al. Continuing evolution of *Burkholderia mallei* through genome reduction and large-scale rearrangements. Genome Biol Evol. 2010; 2:102–16. Epub 2010/03/25. https://doi.org/10.1093/gbe/evq003 PMID: 20333227; PubMed Central PMCID: PMC2839346.
8. Li X-Z, Plésiat P, Nikaido H. The challenge of efflux-mediated antibiotic resistance in Gram-negative bacteria. Clin Microbiol Rev. 2015; 28(2):337–418. https://doi.org/10.1128/CMR.00117-14 PMID: 25788514; PubMed Central PMCID: PMC4402952.
9. Rhodes KA, Schweizer HP. Antibiotic resistance in *Burkholderia* species. Drug Resist Updat. 2016; 28:82–90. Epub 2016/09/14. https://doi.org/10.1016/j.drup.2016.07.003 PMID: 27620956; PubMed Central PMCID: PMC5022785.
10. Sarovich DS, Webb JR, Pitman MC, Viberg LT, Mayo M, Baird RW, et al. Raising the Stakes: Loss of efflux pump regulation decreases meropenem susceptibility in *Burkholderia pseudomallei*. Clin Infect Dis. 2018; 67(2):243–50. Epub 2018/02/03. https://doi.org/10.1093/cid/ciy069 PMID: 29394337.
11. Guglierame P, Pasca MR, De Rossi E, Buroni S, Arrigo P, Manina G, et al. Efflux pump genes of the resistance-nodulation-division family in *Burkholderia cenocepacia* genome. BMC Microbiology. 2006; 6:66–. https://doi.org/10.1186/1471-2180-6-66 PMID: 16857052; PubMed Central PMCID: PMC1557404.
12. Podnecky NL, Rhodes KA, Schweizer HP. Efflux pump-mediated drug resistance in *Burkholderia*. Front Microbiol. 2015; 6:305. Epub 2015/04/14. https://doi.org/10.3389/fmicb.2015.00305 PMID: 25926825; PubMed Central PMCID: PMC4396416.
13. Vargiu AV, Pos KM, Poole K, Nikaido H. Editorial: Bad bugs in the XXIst century: Resistance mediated by multi-drug efflux pumps in Gram-negative bacteria. Front Microbiol. 2016; 7:833. Epub 2016/06/16. https://doi.org/10.3389/fmicb.2016.00833 PMID: 27303401; PubMed Central PMCID: PMC4885826.
14. Piddock LJ. Multidrug-resistance efflux pumps—not just for resistance. Nat Rev Microbiol. 2006; 4 (8):629–36. Epub 2006/07/18. https://doi.org/10.1038/nrmicro1464 PMID: 16845433.
15. Bachert BA, Choi SJ, Snyder AK, Rio RVM, Durney BC, Holland LA, et al. A unique set of the *Burkholderia* collagen-like proteins provides insight into pathogenesis, genome evolution and niche adaptation, and infection detection. PLoS ONE. 2015; 10(9):e0137578. Epub 2015/09/15. https://doi.org/10.1371/journal.pone.0137578 PMID: 26356298; PubMed Central PMCID: PMC4565658.
16. Ramachandran GN. Stereochemistry of collagen. Int J Pept Protein Res. 1988; 31(1):1–16. Epub 1988/01/01. PMID: 3284833.
17. Utsumi R, Yagi T, Katayama S, Katsuragi K, Tachibana K, Toyoda H, et al. Molecular cloning and characterization of the fusaric acid-resistance gene from *Pseudomonas cepacia*. Agr Biol Chem. 1991; 55 (7):1913–8. Epub 2014/09/08. https://doi.org/10.1271/bbb1961.55.1913 PMID: 1370369.
18. Toyoda H, Katsuragi K, Tamai T, Ouchi S. DNA sequence of genes for detoxification of fusaric acid, a wilt-inducing agent produced by *Fusarium* species. J Phytopathology. 1991; 133(4):265–77. https://doi.org/10.1111/j.1439-0434.1991.tb00162.x PMID: 002064443.
19. Propst KL, Mima T, Choi K-H, Dow SW, Schweizer HP. A *Burkholderia pseudomallei* Δ*purM* mutant is avirulent in immunocompetent and immunodeficient animals: candidate strain for exclusion from select-agent lists. Infect Immun. 2010; 78(7):3136–43. https://doi.org/10.1128/IAI.01313-09 PMID: 20404077; PubMed Central PMCID: PMC2897367.
20. Hatcher CL, Mott TM, Muruato LA, Sbrana E, Torres AG. *Burkholderia mallei* CLH001 attenuated vaccine strain is immunogenic and protects against acute respiratory glanders. Infection and Immunity. 2016; 84(8):2345–54. https://doi.org/10.1128/IAI.00328-16 PMID: 27271739; PubMed Central PMCID: PMC4962637.
21. Choi KH, Schweizer HP. mini-Tn7 insertion in bacteria with single attTn7 sites: example *Pseudomonas aeruginosa*. Nat Protoc. 2006; 1(1):153–61. Epub 2007/04/05. https://doi.org/10.1038/nprot.2006.24 PMID: 17406227.

22. Hamad MA, Zajdowicz SL, Holmes RK, Voskuil MI. An allelic exchange system for compliant genetic manipulation of the select agents *Burkholderia pseudomallei* and *Burkholderia mallei*. Gene. 2009; 430 (1):123–31. https://doi.org/10.1016/j.gene.2008.10.011 PMID: 19010402; PubMed Central PMCID: PMC2646673.

23. Price EP, Viberg LT, Kidd TJ, Bell SC, Currie BJ, Sarovich DS. Transcriptomic analysis of longitudinal *Burkholderia pseudomallei* infecting the cystic fibrosis lung. Microb Genom. 2018; 4(8):e000194. Epub 2018/07/10. https://doi.org/10.1099/mgen.0.000194 PMID: 29989529.

24. Chan PP, Holmes AD, Smith AM, Tran D, Lowe TM. The UCSC Archaeal Genome Browser: 2012 update. Nucleic Acids Res. 2012; 40(Database issue):D646–52. Epub 2011/11/15. https://doi.org/10.1093/nar/gkr990 PMID: 22080555; PubMed Central PMCID: PMC3245099.

25. Langdon WB. Performance of genetic programming optimised Bowtie2 on genome comparison and analytic testing (GCAT) benchmarks. BioData Min. 2015; 8(1):1. Epub 2015/01/27. https://doi.org/10.1186/s13040-014-0034-0 PMID: 25621011; PubMed Central PMCID: PMC4304608.

26. Solovyev V SA. Automatic annotation of microbial genomes and metagenomic sequences. Metagenomics and its applications in agriculture, biomedicine and environmental studies. 2011:61–78.

27. Hu GQ, Zheng X, Zhu HQ, She ZS. Prediction of translation initiation site for microbial genomes with TriTISA. Bioinformatics. 2009; 25(1):123–5. Epub 2008/11/19. https://doi.org/10.1093/bioinformatics/btn576 PMID: 19015130.

28. Hu GQ, Zheng X, Yang YF, Ortet P, She ZS, Zhu H. ProTISA: a comprehensive resource for translation initiation site annotation in prokaryotic genomes. Nucleic Acids Res. 2008; 36(Database issue):D114–9. Epub 2007/10/19. https://doi.org/10.1093/nar/gkm799 PMID: 17942412; PubMed Central PMCID: PMC2238952.

29. Münch R, Hiller K, Grote A, Scheer M, Klein J, Schobert M, et al. Virtual Footprint and PRODORIC: an integrative framework for regulon prediction in prokaryotes. Bioinformatics. 2005; 21(22):4187–9. Epub 2005/08/20. https://doi.org/10.1093/bioinformatics/bti635 PMID: 16109747.

30. McNitt DH, Choi SJ, Keene DR, Van De Water L, Squeglia F, Berisio R, et al. Surface-exposed loops and an acidic patch in the Scl1 protein of group A *Streptococcus* enable Scl1 binding to wound-associated fibronectin. J Biol Chem. 2018; 293(20):7796–810. https://doi.org/10.1074/jbc.RA118.002250 PMID: 29615492

31. Caswell CC, Oliver-Kozup H, Han R, Lukomska E, Lukomski S. Scl1, the multifunctional adhesin of group A *Streptococcus*, selectively binds cellular fibronectin and laminin, and mediates pathogen internalization by human cells. FEMS Microbiol Lett. 2010; 303(1):61–8. Epub 2009/12/17. https://doi.org/10.1111/j.1574-6968.2009.01864.x PMID: 20002194; PubMed Central PMCID: PMC2910189.

32. Benjamin W, Andrej S. Comparative Protein Structure Modeling Using MODELLER. Current Protocols in Bioinformatics. 2014; 47(1):5.6.1–5.6.32. https://doi.org/10.1002/0471250953.bi0506s47 PMID: 25199792.

33. Berisio R, Vitagliano L, Mazzarella L, Zagari A. Crystal structure of the collagen triple helix model [(Pro-Pro-Gly)$_{10}$]$_3$. Protein Sci. 2002; 11(2):262–70. Epub 2002/01/16. https://doi.org/10.1110/ps.32602 PMID: 11790836; PubMed Central PMCID: PMC2373432.

34. Yahyavi M, Falsafi-Zadeh S, Karimi Z, Kalatarian G, Galehdari H. VMD-SS: A graphical user interface plug-in to calculate the protein secondary structure in VMD program. Bioinformation. 2014; 10(8):548–50. Epub 2014/09/27. https://doi.org/10.6026/97320630010548 PMID: 25258493; PubMed Central PMCID: PMC4166777.

35. Pettersen EF, Goddard TD, Huang CC, Couch GS, Greenblatt DM, Meng EC, et al. UCSF Chimera—a visualization system for exploratory research and analysis. J Comput Chem. 2004; 25(13):1605–12. Epub 2004/07/21. https://doi.org/10.1002/jcc.20084 PMID: 15264254.

36. Quoilin S, Lambion N, Mak R, Denis O, Lammens C, Struelens M, et al. Soft tissue infections in Belgian rugby players due to *Streptococcus pyogenes* emm type 81. Euro Surveill. 2006; 11(12):E061221.2. https://doi.org/10.2807/esw.11.51.03099-en PMID: 17213570

37. Sirijant N, Sermswan RW, Wongratanacheewin S. *Burkholderia pseudomallei* resistance to antibiotics in biofilm-induced conditions is related to efflux pumps. J Med Microbiol. 2016; 65(11):1296–306. https://doi.org/10.1099/jmm.0.000358 PMID: 27702426.

38. Rv R. Fungal Sensing: iGEM Wageningen UR 2014; 2014. Available from: http://2014.igem.org/Team:Wageningen_UR/project/fungal_sensing.

39. Crutcher FK, Puckhaber LS, Stipanovic RD, Bell AA, Nichols RL, Lawrence KS, et al. Microbial resistance mechanisms to the antibiotic and phytotoxin fusaric acid. J Chem Ecol. 2017; 43(10):996–1006. https://doi.org/10.1007/s10886-017-0889-x PMID: 28986689.

40. Van Dyk TK, Templeton LJ, Cantera KA, Sharpe PL, Sariaslani FS. Characterization of the *Escherichia coli* AaeAB efflux pump: a metabolic relief valve? J Bacteriol. 2004; 186(21):7196–204. Epub 2004/10/

19. https://doi.org/10.1128/JB.186.21.7196-7204.2004 PMID: 15489430; PubMed Central PMCID: PMC523213.

41. Thibault FM, Hernandez E, Vidal DR, Girardet M, Cavallo J-D. Antibiotic susceptibility of 65 isolates of *Burkholderia pseudomallei* and *Burkholderia mallei* to 35 antimicrobial agents. J Antimicrob Chemother. 2004; 54(6):1134–8. https://doi.org/10.1093/jac/dkh471 PMID: 15509614.

42. Xu Y, Keene DR, Bujnicki JM, Höök M, Lukomski S. Streptococcal Scl1 and Scl2 proteins form collagen-like triple helices. J Biol Chem. 2002; 277(30):27312–8. Epub 2002/04/27. https://doi.org/10.1074/jbc.M201163200 PMID: 11976327.

43. Brodsky-Doyle B, Leonard KR, Reid KB. Circular-dichroism and electron-microscopy studies of human subcomponent C1q before and after limited proteolysis by pepsin. Biochem J. 1976; 159(2):279–86. https://doi.org/10.1042/bj1590279 PMID: 187173

44. Duncan C, Prashar A, So J, Tang P, Low DE, Terebiznik M, et al. Lcl of *Legionella pneumophila* is an immunogenic GAG binding adhesin that promotes interactions with lung epithelial cells and plays a crucial role in biofilm formation. Infect Immun. 2011; 79(6):2168–81. Epub 2011/03/23. https://doi.org/10.1128/IAI.01304-10 PMID: 21422183; PubMed Central PMCID: PMC3125840.

45. Paterson GK, Nieminen L, Jefferies JMC, Mitchell TJ. PclA, a pneumococcal collagen-like protein with selected strain distribution, contributes to adherence and invasion of host cells. FEMS Microbiol Lett. 2008; 285(2):170–6. https://doi.org/10.1111/j.1574-6968.2008.01217.x PMID: 18557785

46. Pizarro-Guajardo M, Olguin-Araneda V, Barra-Carrasco J, Brito-Silva C, Sarker MR, Paredes-Sabja D. Characterization of the collagen-like exosporium protein, BclA1, of *Clostridium difficile* spores. Anaerobe. 2014; 25:18–30. Epub 2013/11/26. https://doi.org/10.1016/j.anaerobe.2013.11.003 PMID: 24269655.

47. Poole K, Gotoh N, Tsujimoto H, Zhao Q, Wada A, Yamasaki T, et al. Overexpression of the mexC-mexD-oprJ efflux operon in nfxB-type multidrug-resistant strains of *Pseudomonas aeruginosa*. Mol Microbiol. 1996; 21(4):713–24. Epub 1996/08/01. https://doi.org/10.1046/j.1365-2958.1996.281397.x PMID: 8878035.

48. Moore RA, DeShazer D, Reckseidler S, Weissman A, Woods DE. Efflux-mediated aminoglycoside and macrolide resistance in *Burkholderia pseudomallei*. Antimicrob Agents Chemother. 1999; 43(3):465–70. Epub 1999/02/27. https://doi.org/10.1128/AAC.43.3.465 PMID: 10049252; PubMed Central PMCID: PMC89145.

49. Poole K, Tetro K, Zhao Q, Neshat S, Heinrichs DE, Bianco N. Expression of the multidrug resistance operon mexA-mexB-oprM in *Pseudomonas aeruginosa*: mexR encodes a regulator of operon expression. Antimicrob Agents Chemother. 1996; 40(9):2021–8. Epub 1996/09/01. https://doi.org/10.1128/AAC.40.9.2021 PMID: 8878574; PubMed Central PMCID: PMC163466.

50. Maddocks SE, Oyston PC. Structure and function of the LysR-type transcriptional regulator (LTTR) family proteins. Microbiology. 2008; 154(Pt 12):3609–23. Epub 2008/12/03. https://doi.org/10.1099/mic.0.2008/022772-0 PMID: 19047729.

51. Nikaido H, Pagès J-M. Broad specificity efflux pumps and their role in multidrug esistance of Gram negative bacteria. FEMS Microbiology Reviews. 2012; 36(2):340–63. https://doi.org/10.1111/j.1574-6976.2011.00290.x PMC3546547. PMID: 21707670

52. Hu R-M, Liao S-T, Huang C-C, Huang Y-W, Yang T-C. An inducible fusaric acid tripartite efflux pump contributes to the fusaric acid resistance in *Stenotrophomonas maltophilia*. PLoS ONE. 2012; 7(12): e51053. https://doi.org/10.1371/journal.pone.0051053 PMID: 23236431; PubMed Central PMCID: PMC3517613.

53. Ooi WF, Ong C, Nandi T, Kreisberg JF, Chua HH, Sun G, et al. The condition-dependent transcriptional landscape of *Burkholderia pseudomallei*. PLoS Genet. 2013; 9(9):e1003795. Epub 2013/09/27. https://doi.org/10.1371/journal.pgen.1003795 PMID: 24068961; PubMed Central PMCID: PMC3772027.

54. Mohs A, Silva T, Yoshida T, Amin R, Lukomski S, Inouye M, et al. Mechanism of stabilization of a bacterial collagen triple helix in the absence of hydroxyproline. J Biol Chem. 2007; 282(41):29757–65. https://doi.org/10.1074/jbc.M703991200 PMID: 17693404

55. Han R, Zwiefka A, Caswell CC, Xu Y, Keene DR, Lukomska E, et al. Assessment of prokaryotic collagen-like sequences derived from streptococcal Scl1 and Scl2 proteins as a source of recombinant GXY polymers. Appl Microbiol Biotechnol. 2006; 72(1):109–15. Epub 2006/03/23. https://doi.org/10.1007/s00253-006-0387-5 PMID: 16552563.

56. Leski TA, Caswell CC, Pawlowski M, Klinke DJ, Bujnicki JM, Hart SJ, et al. Identification and classification of *bcl* genes and proteins of *Bacillus cereus* group organisms and their application in *Bacillus anthracis* detection and fingerprinting. Appl Environ Microbiol. 2009; 75(22):7163–72. Epub 2009/09/22. https://doi.org/10.1128/AEM.01069-09 PMID: 19767469; PubMed Central PMCID: PMC2786505.

57. Sylvestre P, Couture-Tosi E, Mock M. Polymorphism in the collagen-like region of the *Bacillus anthracis* BclA protein leads to variation in exosporium filament length. J Bacteriol. 2003; 185(5):1555–63. Epub

2003/02/20. https://doi.org/10.1128/jb.185.5.1555-1563.2003 PMID: 12591872; PubMed Central PMCID: PMC148075.

58. Persikov AV, Ramshaw JAM, Brodsky B. Prediction of collagen stability from amino acid sequence. J Biol Chem. 2005; 280(19):19343–9. https://doi.org/10.1074/jbc.M501657200 PMID: 15753081

59. Gu C, Jenkins SA, Xue Q, Xu Y. Activation of the classical complement pathway by *Bacillus anthracis* is the primary mechanism for spore phagocytosis and involves the spore surface protein BclA. J Immunol. 2012; 188(9):4421–31. Epub 2012/03/24. https://doi.org/10.4049/jimmunol.1102092 PMID: 22442442; PubMed Central PMCID: PMC3331890.

60. Herrick S, Blanc-Brude O, Gray A, Laurent G. Fibrinogen. Int J Biochem Cell Biol. 1999; 31(7):741–6. Epub 1999/09/01. https://doi.org/10.1016/s1357-2725(99)00032-1 PMID: 10467729.

61. Vaudaux P, Pittet D, Haeberli A, Huggler E, Nydegger UE, Lew DP, et al. Host factors selectively increase staphylococcal adherence on inserted catheters: a role for fibronectin and fibrinogen or fibrin. J Infect Dis. 1989; 160(5):865–75. Epub 1989/11/01. https://doi.org/10.1093/infdis/160.5.865 PMID: 2809259.

62. Ko YP, Flick MJ. Fibrinogen is at the interface of host defense and pathogen virulence in *Staphylococcus aureus* infection. Semin Thromb Hemost. 2016; 42(4):408–21. Epub 2016/04/09. https://doi.org/10.1055/s-0036-1579635 PMID: 27056151; PubMed Central PMCID: PMC5514417.

63. Fitzgerald JR, Loughman A, Keane F, Brennan M, Knobel M, Higgins J, et al. Fibronectin-binding proteins of *Staphylococcus aureus* mediate activation of human platelets via fibrinogen and fibronectin bridges to integrin GPIIb/IIIa and IgG binding to the FcgammaRIIa receptor. Mol Microbiol. 2006; 59 (1):212–30. Epub 2005/12/20. https://doi.org/10.1111/j.1365-2958.2005.04922.x PMID: 16359330.

64. Rhodes KA, Somprasong N, Podnecky NL, Mima T, Chirakul S, Schweizer HP. Molecular determinants of *Burkholderia pseudomallei* BpeEF-OprC efflux pump expression. Microbiology. 2018; 164(9):1156–67. Epub 2018/07/20. https://doi.org/10.1099/mic.0.000691 PMID: 30024368; PubMed Central PMCID: PMC6230764.

65. Teelucksingh T, Thompson LK, Cox G. The evolutionary conservation of *Escherichia coli* drug efflux pumps supports physiological functions. J Bacteriol. 2020; 202(22). Epub 2020/08/26. https://doi.org/10.1128/JB.00367-20 PMID: 32839176.

66. Crutcher FK, Liu J, Puckhaber LS, Stipanovic RD, Bell AA, Nichols RL. FUBT, a putative MFS transporter, promotes secretion of fusaric acid in the cotton pathogen *Fusarium oxysporum f. sp. vasinfectum*. Microbiology. 2015; 161(Pt 4):875–83. Epub 2015/01/30. https://doi.org/10.1099/mic.0.000043 PMID: 25627440.

67. Madej MG. Function, structure, and evolution of the major facilitator superfamily: The LacY manifesto. Advances in Biology. 2014; 2014(Article ID 523591):20. https://doi.org/10.1155/2014/523591.

68. Pasqua M, Grossi M, Zennaro A, Fanelli G, Micheli G, Barras F, et al. The varied role of efflux pumps of the MFS family in the interplay of bacteria with animal and plant cells. Microorganisms. 2019; 7(9). Epub 2019/08/25. https://doi.org/10.3390/microorganisms7090285 PMID: 31443538; PubMed Central PMCID: PMC6780985.

69. Hinchliffe P, Greene NP, Paterson NG, Crow A, Hughes C, Koronakis V. Structure of the periplasmic adaptor protein from a major facilitator superfamily (MFS) multidrug efflux pump. FEBS Lett. 2014; 588 (17):3147–53. Epub 2014/07/06. https://doi.org/10.1016/j.febslet.2014.06.055 PMID: 24996185; PubMed Central PMCID: PMC4158417.

70. Tornroth-Horsefield S, Gourdon P, Horsefield R, Brive L, Yamamoto N, Mori H, et al. Crystal structure of AcrB in complex with a single transmembrane subunit reveals another twist. Structure. 2007; 15 (12):1663–73. Epub 2007/12/13. https://doi.org/10.1016/j.str.2007.09.023 PMID: 18073115.

71. Wang Z, Fan G, Hryc CF, Blaza JN, Serysheva II, Schmid MF, et al. An allosteric transport mechanism for the AcrAB-TolC multidrug efflux pump. Elife. 2017; 6. Epub 2017/03/30. https://doi.org/10.7554/eLife.24905 PMID: 28355133; PubMed Central PMCID: PMC5404916.

72. Hobbs EC, Yin X, Paul BJ, Astarita JL, Storz G. Conserved small protein associates with the multidrug efflux pump AcrB and differentially affects antibiotic resistance. Proc Natl Acad Sci U S A. 2012; 109 (41):16696–701. Epub 2012/09/27. https://doi.org/10.1073/pnas.1210093109 PMID: 23010927; PubMed Central PMCID: PMC3478662.

73. Delmar JA, Su CC, Yu EW. Bacterial multidrug efflux transporters. Annu Rev Biophys. 2014; 43:93–117. Epub 2014/04/08. https://doi.org/10.1146/annurev-biophys-051013-022855 PMID: 24702006; PubMed Central PMCID: PMC4769028.

74. Loftin IR, Franke S, Roberts SA, Weichsel A, Heroux A, Montfort WR, et al. A novel copper-binding fold for the periplasmic copper resistance protein CusF. Biochemistry. 2005; 44(31):10533–40. Epub 2005/08/03. https://doi.org/10.1021/bi050827b PMID: 16060662.

75. Loftin IR, Franke S, Blackburn NJ, McEvoy MM. Unusual Cu(I)/Ag(I) coordination of *Escherichia coli* CusF as revealed by atomic resolution crystallography and X-ray absorption spectroscopy. Protein Sci.

2007; 16(10):2287–93. Epub 2007/09/26. https://doi.org/10.1110/ps.073021307 PMID: 17893365; PubMed Central PMCID: PMC2204137.

76. Huang YW, Hu RM, Yang TC. Role of the *pcm-tolCsm* operon in the multidrug resistance of *Stenotrophomonas maltophilia*. J Antimicrob Chemother. 2013; 68(9):1987–93. Epub 2013/05/01. https://doi.org/10.1093/jac/dkt148 PMID: 23629016.

77. Quecine MC, Kidarsa TA, Goebel NC, Shaffer BT, Henkels MD, Zabriskie TM, et al. An interspecies signaling system mediated by fusaric acid has parallel effects on antifungal metabolite production by *Pseudomonas protegens* strain Pf-5 and antibiosis of *Fusarium spp*. Appl Environ Microbiol. 2015; 82 (5):1372–82. Epub 2015/12/15. https://doi.org/10.1128/AEM.02574-15 PMID: 26655755; PubMed Central PMCID: PMC4771327.

78. Tung TT, Jakobsen TH, Dao TT, Fuglsang AT, Givskov M, Christensen SB, et al. Fusaric acid and analogues as Gram-negative bacterial quorum sensing inhibitors. Eur J Med Chem. 2017; 126:1011–20. https://doi.org/10.1016/j.ejmech.2016.11.044 PMID: 28033578

79. Ruiz J, M Bernar E, Jung K. Production of siderophores increases resistance to fusaric acid in Pseudomonas protegens Pf-52015. e0117040 p.

80. van Rij ET, Girard G, Lugtenberg BJJ, Bloemberg GV. Influence of fusaric acid on phenazine-1-carboxamide synthesis and gene expression of *Pseudomonas chlororaphis* strain PCL1391. Microbiology. 2005; 151(Pt 8):2805–14. Epub 2005/08/05. https://doi.org/10.1099/mic.0.28063-0 PMID: 16079356.